THE JOURNAL
OF
CHEMICAL PHYSICS

VOLUME 10 NOVEMBER, 1942 NUMBER 11

The Long Wave-Length Spectra of Saturated Carboxylic Acids, Esters, and Salts

HENRY L. MCMURRY
Department of Physics, Rensselaer Polytechnic Institute, Troy, New York

(Received July 30, 1942)

Electron configurations for the low excited states of the COOR radical (R = alkyl group or H atom) and the COO^- ion are given. Their longest wave-length absorptions are interpreted in terms of transitions to their lowest excited states. In the COOR radical this absorption comes at λ2100 and is weak. It is interpreted as due to a transition like that producing the weak region at λ2900 in the spectrum of the >C=O group in aldehydes and ketones. The COO^- ion appears to show an analogous weak absorption but this is largely covered by a much stronger region. The latter is interpreted as possibly due to a transition in which a non-bonding oxygen electron is excited to an antibonding molecular orbital of the unsaturation or *x* type. This transition should be strong in the ion, probably is weak in the acids and esters, and is entirely absent in the aldehydes and ketones. Possible interpretations of the λ1700 absorption in acids and esters are briefly discussed.

I. INTRODUCTION

THE longest wave-length absorption regions characteristic of saturated molecules containing the >C=O, COOR, and COO^- groups are shown in Fig. 1. In all saturated carboxylic acids and esters there is a weak region with a maximum near λ2100.[1–3] Since the absorption must arise from parts of the molecules having nearly identical electronic structures, it can be attributed to the carboxyl group. One is also led to expect such a weak absorption at long wave-lengths for the carboxyl group, since the longest wave-length absorption from the carbonyl (>C=O) group at λ2900 is weak.[4]

In the acids and esters the weak absorption merges into a stronger region with a maximum near λ1700.[1] This absorption is ten or more times stronger than that at λ2100.[5]

The spectrum of the carboxyl ion can be obtained by dissolving the easily ionized alkali salts of the saturated acids in water.[2,6] The absorption then begins at somewhat shorter wave-lengths than for the acids and rises rapidly without showing any maximum within the range

[1] G. Scheibe, F. Povenz, and C. F. Linström, Zeits. f. physik. Chemie **B20**, 297 (1933).
[2] H. Ley and B. Arends, Zeits. f. physik. Chemie **B17**, 177 (1932).
[3] J. Bielecki and V. Henri, Ber. d. D. Chem. Ges. **46**, 1304 (1913).
[4] See H. L. McMurry, J. Chem. Phys. **9**, 231 (1941) for a discussion.

[5] The *f* values for the λ1700 and λ2100 absorptions in the vapor as estimated from the curves of Scheibe *et al.* (reference 1, Fig. 7) come out about 0.02 and 0.002, respectively. The *f* value for the λ2100 absorption of the pure liquids or the solutions of the compounds is also about 0.002 (reference 2). The absorption curves for the λ1700 regions have not been measured beyond their maxima. The estimated *f* value, which depends on the width of the region at half the maximum intensity, is less reliable for the λ1700 regions than for the others. See reference 4 for the method of estimating *f* values.

[6] Although the ionization constants for the acids are small, an appreciable number of carboxyl ions can be obtained in very dilute water solutions of these materials. With long path lengths their absorptions should be like those of the salts. Formic and succinic acids have relatively high ionization constants and should be suitable for such an experiment. Experiments like this have been done with salicylic acid (a conjugated acid). See C. Shin-Piaw and C. Fabry, Comptes rendus **208**, 292, 1563 (1939).

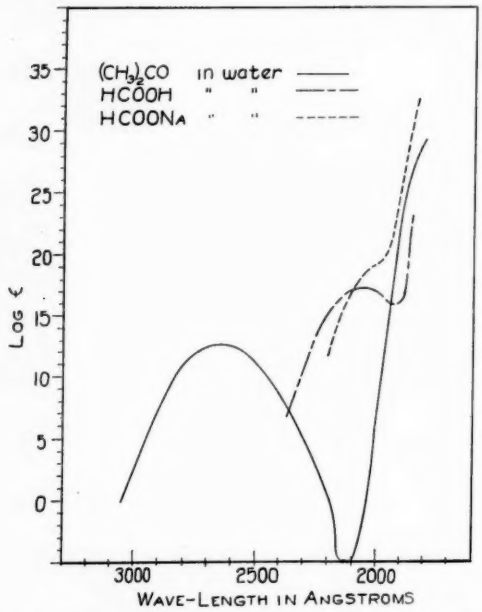

FIG. 1. Absorption regions characteristic of the >C=O, COOR, and COO^- groups. These curves are based on data and absorption curves given by Ley and Arends in reference 2 and also in Zeits. f. physik. Chemie **B12**, 132 (1931). In the vapor the HCOOH absorption below λ2000 shows a maximum around λ1700 where log $\epsilon=3.0$ (see reference 1).

of observations.[2] The curves (see Fig. 1) suggest that this absorption may have a higher intensity than the λ1700 region in the acids. Its maximum is very possibly at somewhat longer wave-lengths than λ1700. The spectra of the ions obtained from several salts show a low intensity shoulder on the long wave-length side of this strong region. Apparently this weak transition, if it is an independent one, has its maximum at shorter wave-lengths than λ2100.

In the following work the electronic structures and spectra of saturated molecules containing the COOR radical or the COO^- ion will be discussed. A similar discussion for molecules in which this radical or ion is conjugated to the rest of the molecule is contemplated for a later article.

II. ELECTRONIC STRUCTURE OF THE COO^- ION AND THE COOR RADICAL IN SATURATED ORGANIC MOLECULES

A. Electron Configurations for the COO^- Ion

The semilocalized molecular orbitals (MO's) for the COO^- ion must belong to representations of the point group[7,8] C_{2v}. Those MO's which are important for the present discussion have forms which may be determined qualitatively by solving the secular equations[9] from which they are derived. They can be described in terms of the axes shown in Fig. 2.

Three types of MO's must be considered. One of these, the "x" type,[10] contains a node in the plane of the group and can be approximated by linear combinations of the $2p_x$ atomic orbitals (AO's) of the three atoms. There are three x MO's denoted here by $\chi_1(b_1)$, $\chi_2(a_2)$, and $\chi_3(b_1)$, where the letters b_1 and a_2 refer to the species of C_{2v} to which the MO's belong. The solutions of the secular equation for these MO's show that χ_1 is O−C−O bonding, χ_2 is non-bonding, and χ_3 is O−C−O antibonding.[11] The second group of

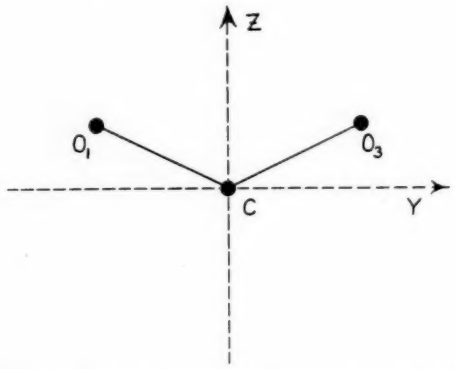

FIG. 2. Axes for COO^-. See reference 8 for details.

[7] See R. S. Mulliken, Phys. Rev. **43**, 279 (1933).

[8] The OCO angle in acids and esters is about 125°, the C−O distances are reported to be about 1.29A. The dimensions in the ion should not be greatly different. See L. Pauling, *The Nature of the Chemical Bond* (Cornell University Press, 1939), p. 188.

[9] If an MO is expressed as a linear combination of all the atomic orbitals (AO's) of the valence electrons in the atoms concerned, a secular equation can be formed by the usual methods of perturbation theory. For atom groups of high symmetry this equation factors into parts each of which gives the forms and energies of the MO's belonging to a particular symmetry class.

[10] H. L. McMurry, J. Chem. Phys. **9**, 241 (1941).

[11] The χ MO's may be expressed by the relation

$$\chi_i=a_ix_1+b_ix_2+c_ix_3,$$

where

$$a_1=c_1>b_1;\quad a_2=-c_2;\quad b_2=0;\quad a_3=c_3\gtrsim -b_3.$$

An MO formed as a linear combination of AO's (LCAO MO) is bonding between two atoms when the positive parts of the AO's of adjacent atoms overlap. It is antibonding when positive and negative parts overlap. These bonding characteristics are weak, essentially non-bonding, whenever the overlapping of adjacent AO's is small, or when one or both AO's appear with a small coefficient in the LCAO expression (see reference 9).

MO's are of the "σ" type with wave functions concentrated along the O−C lines. These can be built by combining suitably oriented $2p$ AO's of the O atoms with properly chosen mixtures of $2p_z$, $2p_y$, and $2s$ AO's of carbon. Two of these MO's designated as $\varphi_1(a_1)$ and $\varphi_2(b_2)$ are O−C bonding while two others, $\psi_1(a_1)$ and $\psi_2(b_2)$, are O−C antibonding.[12] Finally, there are two MO's, denoted here by $\omega_1(a_1)$ and $\omega_2(b_2)$, which are expected to exhibit the same non-bonding character that distinguishes the closely analogous y_0 MO in aldehydes and ketones.[4] They can be constructed primarily from $2p$ AO's of the O_3 and O_1 atoms with symmetry axes in the plane of the molecule perpendicular to the O_3-C and O_1-C lines, respectively.[14] These oxygen AO's will hereafter be denoted by q_3 and q_1, respectively.

The electron configurations for the normal and low excited states of the COO^- ion are given below in what is later estimated to be the order of increasing energy. The species symbol is used wherever an MO appears.

$$\begin{array}{llllllll}
N\text{—}\varphi_1^2(a_1) & \varphi_2^2(b_2) & \chi_1^2(b_1) & \omega_1^2(a_1) & \chi_2^2(a_2) & \omega_2^2(b_2), & & {}^1A_1. \\
E_1\text{—}\varphi_1^2(a_1) & \varphi_2^2(b_2) & \chi_1^2(b_1) & \omega_1^2(a_1) & \chi_2^2(a_2) & \omega_2(b_2) & \chi_3(b_1), & {}^{3,1}A_2. \\
X\text{—}\varphi_1^2(a_1) & \varphi_2^2(b_2) & \chi_1^2(b_1) & \omega_1^2(a_1) & \chi_2(a_2) & \omega_2^2(b_2) & \chi_3(b_1), & {}^{3,1}B_2. \\
E_2\text{—}\varphi_1^2(a_1) & \varphi_2^2(b_2) & \chi_1^2(b_1) & \omega_1(a_1) & \chi_2^2(a_2) & \omega_2^2(b_2) & \chi_3(b_1), & {}^{3,1}B_1.
\end{array} \qquad (1)$$

In aldehydes and ketones the lowest excited MO is of the x type.[4,10] This has also been assumed to be true for the analogous χ_3 MO in (1). The ω_1 MO is possibly slightly O−C−O bonding and has been placed lower than the χ_2 MO which is almost entirely localized on the oxygen atoms[11] and therefore must be almost completely non-bonding. The evidence discussed below makes it seem probable that the absorption at longest wave-lengths in the ion can come only from excitation of either an ω_1 or an ω_2 electron. For this reason ω_2 has been given the highest energy of any MO used in (1). It is probably slightly antibonding.

The longest wave-length absorption in the ion[2] has a strong maximum below λ1850 and carries a shoulder on its long wave-length side indicating that a weak region possibly is present around λ1900–λ2000. These features can be explained in terms of the configurations used in (1). Theoretical intensity calculations[13] show that the $N\rightarrow E_1$ transition is of the forbidden type while $N\rightarrow E_2$ must have a very low intensity. Both of these transitions can obtain some intensity from electronic-vibrational coupling[15] but at best are expected to be weak. In contrast with these low intensities, that predicted for the $N\rightarrow X$ transition is very large.[16] On the basis of these predicted intensities it is logical to assign the weak region which apparently comes around λ2000 to the $N\rightarrow E_1$ transition and the strong region following this to the $N\rightarrow X$ transition. The weak $N\rightarrow E_2$ transition must lie underneath the $N\rightarrow X$ region or may come at still shorter wave-lengths.

The positions observed for the $N\rightarrow X$ and the $N\rightarrow E_1$ absorptions in the COO^- ion relative to the corresponding weak absorption at λ2900 in aldehydes and ketones can, in part, be explained by the fact that the oxygen atom in aldehydes and ketones has more negative charge than either of the oxygen atoms in the ion. The excited MO may also have a somewhat higher energy in the ion than in the aldehydes and ketones. These facts will be discussed further in a later paragraph.

[12] There is evidence for believing φ_1 and φ_2, and also ψ_1 and ψ_2, are nearly degenerate (reference 10, footnote 11). This means that localized MO's are appropriate for describing the O_1-C and O_3-C σ bonds. Since interaction between these localized MO's must be small, the semi-localized MO's φ_1 and φ_2 can be approximated by respectively taking positive and negative linear combinations of the localized bonding MO's of the O_1-C and O_3-C bonds. Similarly ψ_1 and ψ_2 can be approximated by taking corresponding combinations of the two antibonding MO's.

[13] These calculations were made in the same way as in eference 4.

[14] The simplest possible LCAO approximations for ω_1 and ω_2 can be written as $(q_1+q_2)/2^{\frac{1}{2}}$ and $(q_1-q_2)/2^{\frac{1}{2}}$, respectively. Better approximations would require the presence of some $2p_z$ and $2s$ of carbon in ω_1 and some $2p_y$ of carbon in ω_2.

[15] G. Herzberg and E. Teller, Zeits. f. physik. Chemie **B21**, 410 (1933); H. Sponer and E. Teller, Rev. Mod. Phys. **13**, 75 (1941).

[16] The calculated value of Q^2 (dipole moment integral) for the $N\rightarrow X$ transition is about $0.7A^2$, that for the $N\rightarrow E_2$ transition about $0.002A^2$.

B. Electron Configurations for the COOR Radical

For discussing the electronic structure of the COOR radical, localized MO's can best be used. The R group will be regarded as attached to the O_3 atom by an MO of the σ type. In the acids, strong hydrogen bonding between the H and O_1 atoms will hold the hydrogen in the OCO plane.[17] In the esters the $R-O_3$ bonding MO may possibly have its axis out of the OCO plane. Configurations for the two cases where this axis lies respectively in and perpendicular to the OCO plane will be discussed. The AO of the R group used in describing the $R-O_3$ bond will always be denoted by σ_R. It behaves like $1s$ of hydrogen or $2p\sigma$ of carbon when R denotes an H atom or an alkyl group, respectively.

In place of the φ_1, φ_2, ψ_1, and ψ_2 MO's of the COO^- ion, four localized MO's of the σ type are now used. Two of these, one bonding and one antibonding, are localized in the O_3-C bond, while a similar pair is localized in the O_1-C bond. The carbon AO's appearing in the LCAO MO expressions for these σ MO's are again linear combinations of $2p_z$, $2p_y$, and $2s$ AO's. The carbon AO's directed toward atoms 1 and 3, respectively, will be denoted by $\sigma_{1,2}$ and $\sigma_{3,2}$. The oxygen AO's with which these combine are denoted by σ_1 and σ_3, respectively.

The MO's localized in the $O_1=C$ part of the radical are very much like their respective counterparts in the carbonyl group.[4] They will be described in essentially the same way as in reference 4 except that now two of the O_1 AO's are denoted by q_1 and σ_1 instead of y_O and z_O, respectively.

Finally, the O_3 atom contains two nearly non-bonding $2p$ electrons with the axes of their wave function perpendicular to both the O_3-C and $R-O_3$ lines.

Wherever possible the letters used below to designate the configurations of the COOR radical have been chosen so that a given state bears the same designation as the state in (1) to which it shows the closest correspondence.

For the case where the $R-O_3$ bonding MO lies in the OCO plane these configurations may be written as follows:

$$\begin{aligned} &N\text{—}(q_3\sigma_R)^2(\sigma_3\sigma_{3,2})^2(\sigma_1\sigma_{1,2})^2(x_1x_2)^2(x_3)^2(q_1)^2.\\ &E_1\text{—}(q_3\sigma_R)^2(\sigma_3\sigma_{3,2})^2(\sigma_1\sigma_{1,2})^2(x_1x_2)^2(x_3)^2(q_1)(x_1\bar{x}_2).\\ &X\text{—}(q_3\sigma_R)^2(\sigma_3\sigma_{3,2})^2(\sigma_1\sigma_{1,2})^2(x_1x_2)^2(x_3)(q_1)^2(x_1\bar{x}_2). \end{aligned} \tag{2}$$

Analogous configurations for the case where the $R-O_3$ line is perpendicular to the OCO plane may be written as follows:

$$\begin{aligned} &N\text{—}(x_3\sigma_R)^2(\sigma_3\sigma_{3,2})^2(\sigma_1\sigma_{1,2})^2(x_1x_2)^2(q_3)^2(q_1)^2.\\ &E_1\text{—}(x_3\sigma_R)^2(\sigma_3\sigma_{3,2})^2(\sigma_1\sigma_{1,2})^2(x_1x_2)^2(q_3)^2(q_1)(x_1\bar{x}_2).\\ &E_2\text{—}(x_3\sigma_R)^2(\sigma_3\sigma_{3,2})^2(\sigma_1\sigma_{1,2})^2(x_1x_2)^2(q_3)(q_1)^2(x_1\bar{x}_2). \end{aligned} \tag{3}$$

Here, as in the previous article,[4] any symbol such as x_1x_2 indicates an MO formed as a linear combination of the two AO's indicated. The bars denote antibonding MO's.

In both of these configurations the lowest excited MO is of the x type and is exactly analogous to the lowest excited MO of the carbonyl group. The non-bonding electrons on the O_1 atom are assumed to have a higher energy than those on the O_3 atom. This is not certain—particularly in the acids where the O_3 atom is able to draw charge from the hydrogen atom. However, this order proves to be unimportant for the interpretation of the spectrum at longest wave-lengths. Similarly the order for the energies of the bonding σ MO's is uncertain. These MO's are not involved in any of the transitions considered here and their energy order does not need to be known.

The configurations given in (2) and (3) are equally capable of explaining the observed absorption of the COOR group. Intensity calculations again show that the longest wave-length absorption should be weak, in agreement with what is observed for the region at λ2100 in all acids and esters. An interesting fact is that the $N\rightarrow X$ transition in (2) is found to have an intensity which depends strongly on the amount of interaction between the x_3 AO and the x_1x_2 and $x_1\bar{x}_2$ MO's. Although the $N\rightarrow X$ intensity must be very strong in the ion where this interaction is at its strongest, it may be weak in the COOR group.

The region at λ1700 in acids and esters can possibly be explained by the $N\rightarrow X$ transition. However, the spectra of aldehyde and ketones show that an absorption characteristic of the $>C=O$ group also occurs in this region. It is

[17] See L. Pauling, reference 9, p. 286.

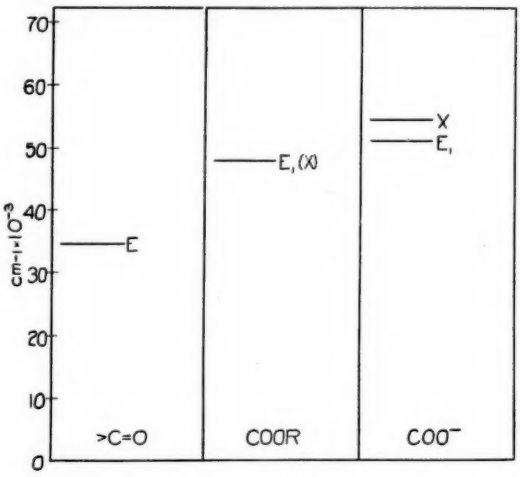

FIG. 3. Energies for the low excited states in >C=O, COOR, and COO^- relative to their normal states. The notation for the states is the same as that used in configurations (1), (2), (3) and in reference 4. The energies for the lowest states have been determined from the longest wave-length absorptions which come, respectively, at λ3000, λ2100, and probably just below λ2100 in >C=O, COOR, and COO^-. The X state in COOR is placed in parenthesis because it very probably may be higher than the E_1 state. The absorption below λ1900 in COO^- is here ascribed to the $N \rightarrow X$ transition. The frequency of its maximum is uncertain but is higher than for the $N \rightarrow E_1$ absorption.

possible that in COOR one or more transitions involving excitation of the non-bonding electrons to MO's of the σ type which are C−O or O_3−R antibonding may well produce this absorption. While these transitions appear to include those most likely to produce the λ1700 absorption, other possibilities exist and an unambiguous assignment does not seem possible at present.

III. COMPARISON OF THE LONGEST WAVE-LENGTH ABSORPTIONS IN >C=O, COOR, AND COO^-

In the normal state of the carbonyl group the carbon is positively, and the oxygen negatively, charged. The presence of the extra oxygen atom (O_3) in the COOR group must cause still more negative charge to leave the carbon. The total charge lost by the carbon is then divided between two oxygen atoms each of which probably has less negative charge than that held by the oxygen of the carbonyl group. As a result the non-bonding electrons should have a higher energy in >C=O than in COOR and perhaps COO^-. In COOR and COO^- the excited x MO is pushed up by interactions between the x_3 AO and the $x_1\bar{x}_2$ MO. In COO^- the x_1 and x_3 AO's are equivalent and this interaction is very strong. It is reasonable to assume that the excited x MO has its highest energy in COO^- and probably its lowest energy in the carbonyl group. These facts show that, if the mechanisms proposed in Part II to explain the longest wave-length absorptions are correct, the absorptions should occur at progressively shorter wave-lengths on going from >C=O to COOR and COO^-. This is observed to be the case, the absorptions coming respectively near λ2900, λ2100, and below λ2000.

In COOR the weak absorption is somewhat stronger than in the carbonyl group. It is possible that the $N \rightarrow X$ absorption, although weak, contributes to this absorption. However, the absorption region next following is about 10,000 cm^{-1} away in COOR and about 15,000 cm^{-1} away in the carbonyl group. The weak absorptions may well steal intensity[15] from these adjacent regions and the situation for doing this is more favorable in COOR.

IV. POSITION OF THE R GROUP IN ESTERS

Theoretically it might be possible to compare the positions and intensities for the absorptions in the acids and esters and thereby determine whether the O−R line in esters had any definite orientation with respect to the OCO plane. However, the data thus far available are not sufficient for this purpose. The broad aspects observed for the longest wave-length absorptions are equally explicable using either configuration (2) or (3). A much more detailed knowledge of the positions and intensities of the absorptions throughout the vacuum regions seems necessary if progress is to be made in this direction.[18]

V. SUMMARY

The evidence presented above makes it appear quite certain that the relatively weak absorption at λ2100 in the COOR group is produced by a transition to the E_1 state in (2) or possibly, in esters, to states somewhat like E_1 and E_2 of (3).

[18] Studies of the infra-red absorptions of esters to determine a possible orientation of the O−R line apparently have not been made. Any tendency toward bonding between the R group and the O_1 atom should affect the C=O vibration. The author is indebted to Mr. R. Schlegel of the University of Illinois for correspondence about this point.

The absorptions at λ1700 can possibly come from excitation of the non-bonding oxygen electrons to MO's of the σ type which are C−O or O−R antibonding. Particular assignments are difficult here since at short wave-lengths the number of transitions occurring in a given region may be large.

In the ion, transitions should occur in roughly the same regions as for the analogous transitions in the COOR group. However, the $N \rightarrow X$ absorption, which apparently is weak in the acids, is now expected to be very strong and probably explains the strong absorption below λ1900 in the ion. A weak shoulder on the long wave-length edge of this region indicates that the $N \rightarrow E_1$ absorption is present where it should be expected. The present state of information does not allow a distinction between configuration (2) and other possible configurations such as (3) to be made for esters.

In Fig. 3 these conclusions are summarized by an energy level diagram. A comparison of the positions of the corresponding states in >C=O, COOR, and COO^- is given in terms of correlations with the available experimental data.

In conclusion the writer wishes to express thanks to Professor R. S. Mulliken for much advice and encouragement.

NOVEMBER, 1942 JOURNAL OF CHEMICAL PHYSICS VOLUME 10

The Infra-Red Spectrum of Furan

LUCY W. PICKETT
Department of Chemistry, Mount Holyoke College, South Hadley, Massachusetts
(Received August 10, 1942)

The infra-red spectrum of furan vapor has been investigated in the region from 500 to 35,000 cm^{-1} with a prism spectrograph using potassium bromide, rocksalt, and fluorite prisms. The data have been compared with those of other investigators and the frequency assignments proposed by Lord and Miller for pyrrole were applied to these data.

INTRODUCTION

THESE measurements of the infra-red spectrum of furan vapor were made several years ago in conjunction with an investigation of its ultraviolet spectrum which has been published.[1] Manzoni-Ansidei[2] has reported the measurement of the infra-red spectrum of liquid furan with a rocksalt prism spectrometer and his results will be shown later for comparison. Raman measurements have been made by a number of investigators[3] with results which are consistent in the main. In spite of careful and extensive studies of the problem of the five-membered ring which have been made by Bonino and by Reitz,[3] no conclusive explanation of the observed spectrum of furan has resulted.

Recently Lord and Miller[4] have made an analysis of the vibrational spectra of pyrrole based on Raman and infra-red measurements of pyrrole and several of its deuterium derivatives. Since the molecular structures of pyrrole and furan are so similar, it seemed of interest now to examine the furan data in the light of the frequency assignments made by Lord and Miller with the twofold purpose of interpreting the furan spectrum and of offering an independent test of these assignments.

EXPERIMENTAL

Preparation and Purification of Furan

Three samples of furan were used in these measurements. The first was kindly supplied by Professor G. B. Kistiakowsky and its preparation and careful purification for measurements of heats of hydrogenation have been described.[5] A second was purchased from Eastman Kodak

[1] L. Pickett, J. Chem. Phys. **8**, 293 (1940).
[2] R. Manzoni-Ansidei and M. Rolla, Atti Accad. Lincei **27**, 410 (1938).
[3] See F. Kohlrausch, *Der Smekel-Raman Effekt* (J. Springer, Berlin, 1938), p. 158, for bibliography.
[4] R. C. Lord and F. A. Miller, J. Chem. Phys. **10**, 328 (1942).
[5] M. A. Dolliver, T. L. Gresham, G. B. Kistiakowsky, E. A. Smith, and W. E. Vaughan, J. Am. Chem. Soc. **60**, 440 (1938).

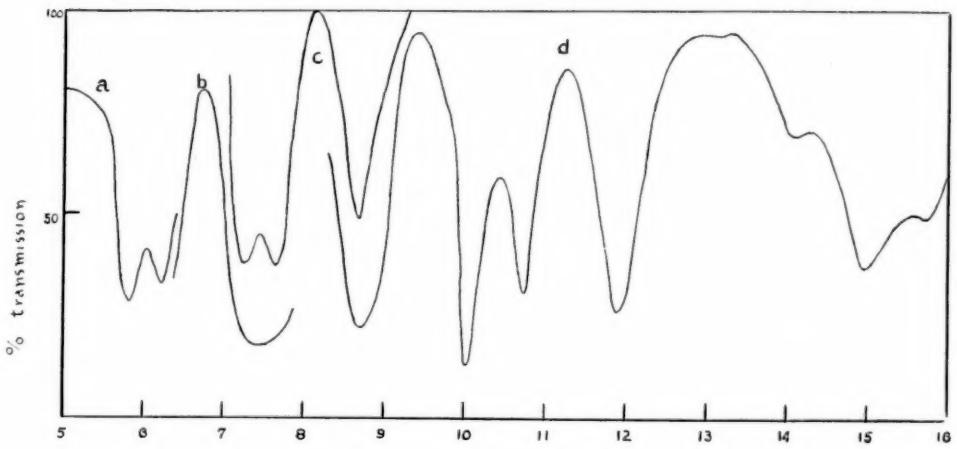

FIG. 1. Infra-red transmission curves for furan vapor. Wave numbers in 100 cm^{-1}.

	Pressure	Prism	Slit width
a.	101 mm	KBr	1.5 mm
b.	347 mm	KBr	1.5 mm
c.	30 mm	KBr	0.75 mm
d.	39 mm	NaCl	0.25–0.5 mm

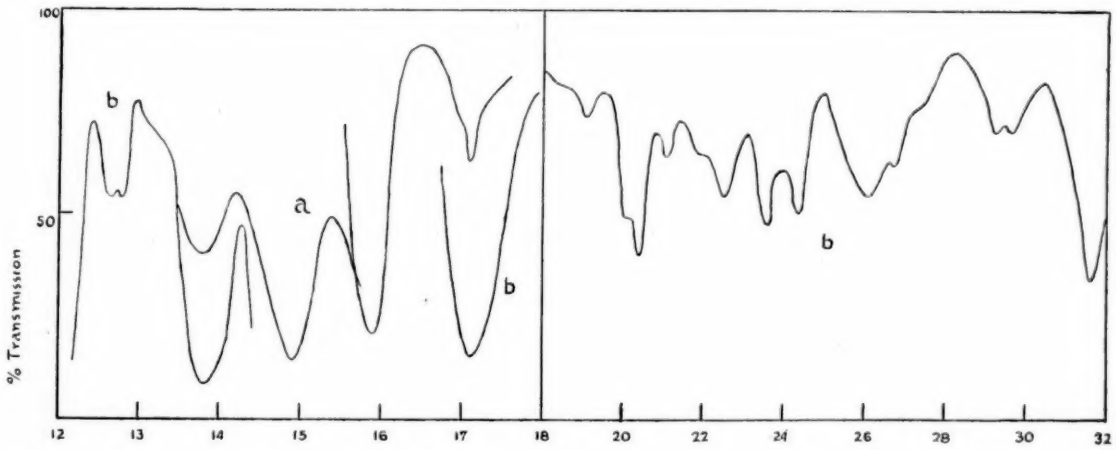

FIG. 2. Infra-red transmission curves of furan vapor using fluorite prism. *a*, pressure = 40 mm; *b*, pressure = 350 mm. slit width 0.1–0.35 mm. Wave number in 100 cm^{-1}.

Company and redistilled through a meter length fractionating column while the third was prepared as described in an earlier reference.[1] All three samples were used for the measurements with the fluorite prism. The first and third were studied with the rocksalt and the first with the potassium bromide prisms. The results obtained from all three were in agreement.

Infra-Red Measurements

The infra-red recording spectrometer at Harvard University which has been previously described[6] was used for the studies through the courtesy of Professor E. B. Wilson, Jr. The absorption of gaseous furan at pressures varying from 10 to 400 mm enclosed in tubes 30 cm long was determined over the region from 2.5 to 20μ using fluorite, rocksalt, and potassium bromide prisms in the appropriate regions of the spectrum. Certain improvements in the sensitivity and steadiness of the spectrometer, which made it possible to use a lower slit width and hence

[6] H. Gershinowitz and E. B. Wilson, Jr., J. Chem. Phys. **6**, 197, 247 (1938).

TABLE I. Frequencies observed for furan (in cm^{-1}).

Infra-red vapor	Infra-red liquid (M−A)	Raman (Reitz)
584 *s*	601 *vs*	601 *dp*
624 *s*	648 *w*	
725 *s*	740 *vs*	724 *p*
763 *s*		839 *dp*
872 *s*	864 *s*	871 *dp*
999 *vs*	990 *vs*	986 *p*
		1034 *dp*
1073 *s*	1052 *w*	1061 *p*
		1137 *p*
1189 *s*	1176 *m*	1171 *dp*
		1200 *p*?
1264 *w*	1249 *w*	1270 *dp*
1277 ?		
1387 *m*	1375 *m*	1380 *p*
		1457 ?
1490 *vs*	1495 *vs*	1483 *p*
1580 *s*		
1694 ?		
1712 *mw*		
1906 *w*		
2012 *vw*		
2040 *mw*		
2105 *w*		
2188 *vw*		
2246 *w*		
2360 *mw*		
2440 *mw*		
2604 *mw*		
2673 *w*		
2730 ?		
2915 *vw*		
2963 *vw*		3089 *p*
3164 *s*		3121 *p*
		3154 *p*

attain higher resolving powers, were made between the first and last measurements. Most of the curves presented were made with the improved apparatus except in the region below 800 cm^{-1} where the resolution with the potassium bromide prism was already excellent. At least four records were made of each part of the spectrum and these were in substantial agreement.

The transmission curves are given in Figs. 1 and 2; the positions of the bands observed are shown in Table I and for comparison, the values obtained by Manzoni-Ansidei from infra-red measurements of the liquid. The wave numbers of the Raman lines with their polarization properties as determined by Reitz[7] are also given. The positions of the Raman lines show a somewhat wide variation as determined by different investigators and have been compared by Reitz.

DISCUSSION OF RESULTS

In comparing the present results with those of other reports, several points would seem to require comment. The table shows that a considerable number of combination and overtone frequencies appear in the region investigated with the fluorite prism which have not been previously observed. Most striking however is the appearance of a strong absorption band at 1580 cm^{-1}. No band of this frequency has been observed in either Raman or infra-red measurements although a vibration frequency of about 1600 cm^{-1} is expected in all compounds with doubly-bonded carbon atoms and its apparent absence in furan has been the subject of much discussion.[3] In the attempt to eliminate the possibility that the band observed here was due to an impurity, the three samples described above were all studied with the fluorite prism in this spectral region and all showed the same intense band. A plausible reason why such a band was not detected in the infra-red measurements made by Manzoni-Ansidei was found when the region was investigated with a rocksalt prism and is evident in Fig. 1. In this the band in question appears only as a shoulder on the side of the stronger band at 1490 cm^{-1} since the dispersion of the rocksalt prism is so much smaller than that of the fluorite in this region.

Two bands which appeared to be single at high pressures were seen to be clearly resolved into two heads each, when sufficiently low pressures were used. Thus the band reported by Manzoni-Ansidei at 601 cm^{-1} shows in these measurements two bands at 584 and 624 cm^{-1} while that at 740 has as its counterpart two at 725 and 763 cm^{-1}. These may be resolved branches of the same band or may represent separate bands.

The values of the present investigation are somewhat higher than those previously observed. The difference is probably to be attributed to the fact that these measurements were of furan vapor whereas all of the others were made on

TABLE II.

	Symmetry elements				No. of vibrations expected				Selection rules
	E	C_{2z}	σ_y*	σ_z	Ring	C−H bending	C−H stretching	Total	Infra-red
A_1	+	+	+	+	4	2	2	8	active
A_2	+	+	−	−	1	2		3	inactive
B_1	+	−	+	−	3	2	2	7	active
B_2	+	−	−	+	1	2		3	active

* σ_y refers to molecular plane.

[7] A. W. Reitz, Zeits. f. physik. Chemie **B38**, 275 (1938).

liquid furan. Crawford and Joyce[8] have noted that in the case of methyl ether the vapor frequencies averaged 20 cm^{-1} higher than those of the liquid.

Assignment of Frequencies

The probable symmetry of the furan molecule is C_{2v}. Schomaker and Pauling[9] have made electron diffraction measurements which give the molecular dimensions and support this view. The classification of frequencies to be expected on the basis of this symmetry is shown in Table II.

The C−H stretching frequencies are above 3000 cm^{-1} and are not resolved in these measurements as the dispersion of the spectrograph is low in this region. The vibrations of class A_2 are inactive in the infra-red and may thus be eliminated from consideration here, leaving fourteen frequencies to be identified.

Lord and Miller[4] in their study of pyrrole and its deuterium derivatives have made assignments for all vibrations observed in their Raman and infra-red measurements and conclude that the assumption of C_{2v} symmetry accounts for the facts in satisfactory manner. Except for those frequencies associated with the N−H linkage, each fundamental vibration of pyrrole or pyrrole-*N*-*d* would be expected to have its counterpart in the furan spectrum with some slight modification of frequency; there would also be differences to be taken into account because the pyrrole measurements were made in liquid state.

Table III gives the assignments proposed by Lord and Miller for pyrrole and in the last column corresponding assignments are made for furan. Such an assignment would account for all the observed bands except that at 584 which, as mentioned above, may be a resolved branch. There is no experimental evidence of three bands which would be expected but these may be superimposed on other bands. There is one serious difficulty in this interpretation, however, in that the Raman line at 986 (corresponding to the infra-red band for furan vapor at 999) was found by Reitz to be polarized[7] and thus would represent a totally symmetrical vibration. Reitz' suggestion that the totally symmetrical ring vibrations in liquid furan have frequencies of 724, 986, 1137, and 1483 cm^{-1} is also supported by the finding of a parallel set of excited state frequencies in the ultraviolet spectrum,[1] where only the A_1 ring frequencies were likely to appear. Therefore the 999 cm^{-1} is thought to represent an A_1 ring frequency, probably concerning the oxygen atom to a large extent. In this case, 1387 cm^{-1} may represent a C−H bending vibration and 1264 cm^{-1} be a frequency of class B_1.

TABLE III.

Class	Vibration type	Pyrrole frequency	Furan frequency
A_1	ring	711	725
	ring	1144	1189
	ring	1384	1387
	ring	1467	1490
	C−H bending	1076	1073
	C−H bending	1237	1264
B_1	ring	647	624
	ring	1418	—
	ring	1530	1580
	C−H bending	1015	999?
	C−H bending	1046	—
B_2	ring	838	872
	C−H bending	768	763
	C−H bending	(1046)	—

It is possible to account for all of the bands observed above 1600 cm^{-1} as overtones or combinations which would be allowed by symmetry rules but the large number of existing possibilities mean that there is no great significance in such assignments.

The author wishes to express appreciation to the Lalor Foundation for the grant which supported this work and to Professor E. B. Wilson, Jr. and his co-workers at Harvard University for the assistance and privileges enjoyed there.

[8] B. L. Crawford and L. Joyce, J. Chem. Phys. **7**, 307 (1939).
[9] V. Schomaker and L. Pauling, J. Am. Chem. Soc. **61**, 1769 (1939).

Infra-Red Spectrum of Polyatomic Molecules

XVI. Methyl-d_3-Chloride and Methyl-d_3-Bromide

HERMANN D. NOETHER
Mallinckrodt Chemical Laboratory, Harvard University, Cambridge, Massachusetts

(Received August 12, 1942)

Methyl-d_3-chloride and methyl-d_3-bromide have been synthesized, their infra-red spectrum in the range from 2.8 to 18μ measured, and a complete assignment of the fundamental frequencies has been given. A modified valence-type potential function including two interaction terms fits the fundamental frequencies of the four molecules CH_3Cl, CD_3Cl, CH_3Br, and CD_3Br to within one percent.

IN connection with the synthesis of methyl-d_3-alcohol-d the deutero-methyl halides were prepared. The ordinary halides and related compounds have been previously thoroughly investigated experimentally as well as theoretically. It was therefore considered of interest to see what agreement could be obtained between theory and experiment for the isotopic molecules.

EXPERIMENTAL PART

The infra-red spectrometer used has been described previously.[1] Fluorite, rocksalt, and potassium bromide prisms were used in the appropriate spectral regions. Glass tubes 30 cm long and 4.4 cm or 2.5 cm in diameter with cleaved rocksalt windows, sealed on with Duco cement or Apiezon wax, were used as absorption cells. For some of the experiments the rocksalt windows had been polished, thus increasing their transmission considerably (*ca.* 25 percent). Blanks were recorded over the whole spectral range.

Preparation of Sample

The methyl-d_3-halides were synthesized from CD_3NO_2 which was prepared from CH_3NO_2 by exchange.[2] CD_3NO_2 was reduced to CD_3NH_2HCl as described by H. Krause.[3] The reduction takes place nearly quantitatively at about 70°C with hydrochloric acid and iron filings, if air is excluded, and the medium is kept acidic to completion of the reaction. By removing CO_2 and O_2 from the water used in the reaction and replacing the air in the reaction vessel by H_2 a yield of CD_3NH_2 of 90 percent and better was obtained. CD_3NH_2 is distilled from the strongly basic solution and collected in HCl. The CD_3NH_2HCl solution was evaporated nearly to dryness and then the benzoyl derivative of the amine was prepared in the usual manner. It was dissolved in ether and reprecipitated with ligroin.[4] The benzoyl methyl amide on heating with PCl_5 (PBr_5) decomposes[5] forming the methyl halides, C_6H_5CN, HCl (HBr), and $POCl_3$ ($POBr_3$). The methyl halide was driven over with a slow stream of N_2, and purified by leading it through 30 and 50 percent KOH solutions and over fused KOH and $CaCl_2$ to remove water, finally freezing it out with a dry-ice mixture. Since the decomposition temperature of the benzoylchlorimid, formed as an intermediate, is higher than the boiling point of $POCl_3$ the latter has to be removed first. For the bromine compound which decomposes below the boiling point of $POBr_3$, this is not necessary. The CD_3-group is stable against exchange, therefore no special precautions for storage need to be taken.

Purity of the Product

From the density measurements of the D_2O before and after the exchange with nitromethane and the distribution coefficient[2] the deuterium content could be calculated. This calculation gave a 95 percent pure CD_3NO_2 assuming only CD_3NO_2 and CH_3NO_2 to be present. Mass-spectrograph analysis by Dr. W. Kennedy,

[1] H. Gershinowitz and E. B. Wilson, Jr., J. Chem. Phys. **6**, 197 (1938).
[2] O. Reitz, Zeits. f. physik. Chemie **A176**, 363 (1936). For details, see T. P. Wilson, to be published.
[3] H. Krause, Chem. Zeitung **40**, 810 (1916).
[4] P. van Romburgh, Rec. Trav. Chim. **4**, 388 (1885). F. E. Dunlap, J. Am. Chem. Soc. **24**, 763 (1902).
[5] H. v. Pechmann, Ber. **28**, 2367 (1895); **33**, 611 (1900); **44**, 1465 (1911).

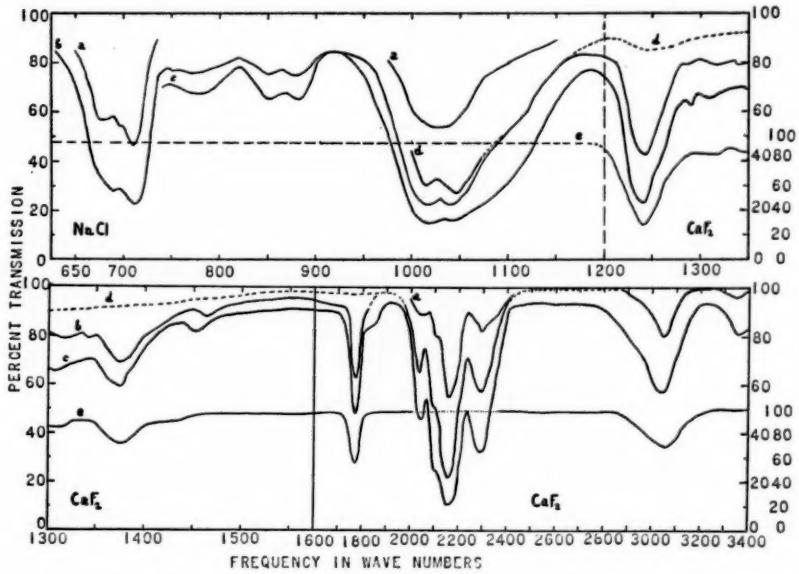

FIG. 1. Absorption spectrum of CD_3Cl. Curves: (*a*) 26 mm Hg; (*b*) ~90 mm Hg; (*c*) 216 mm Hg; (*d*) bands of the purified CD_3Cl (~80 mm Hg) coincide in the C−D and C−H stretch ranges with the 90 mm Hg bands of (*b*) – – – – – visually from records. (*e*) bands of the impurity at ~5 mm Hg (transmission scale ½ normal scale).

who determined the CD_2HNO_2 content to be about 12 percent, checks the above calculation. The nitromethane had been provided specially by the Commercial Solvents Corporation and was distilled through a fractionating column, retaining only the middle fraction.

TABLE I. Frequencies, intensities, and assignment of CD_3Cl bands.

Frequency in cm^{-1}	Int.	Assignment	Frequency in cm^{-1}	Int.	Assignment
680, 695, 711	S	P, Q, R $\nu C-Cl(\pi)$	1240	S	impurity
775	W	$^2\tau(\sigma)$	1310	V. W.	imp.
855	W	? CD_2HCl	1373	M	imp.
881	W	? CD_2HCl	1452	V. W.	CD_2HCl
1016, 1029, 1043	S	P, Q, R $\delta(\pi)$	1764	M	imp.
1050–1060	M	$^2\delta(\sigma)$	2040	M	$2\delta(\pi)$
			2104	M	$2^2\delta(\sigma), \nu(\pi)$
			2162	V. S.	
			2287	S	$^2\nu(\sigma)$
			3043	M	CD_2HCl+imp.
			3368	W	$^2\nu(\sigma)+{}^2\delta(\sigma)$

TABLE II. Frequencies, intensities, and assignment of CD_3Br bands.

Frequency in cm^{-1}	Int.	Assignment	Frequency in cm^{-1}	Int.	Assignment
566, 577, 588	S	P, Q, R $\nu C-Br(\pi)$	1239	S	imp.
717	M	$^2\tau(\sigma)$	1308	V. W.	imp.
790	W	CD_2HBr?	1377	M	imp.
978, 987, 999	S	P, Q, R $\delta(\pi)$	1455	W	CD_2HBr
1053	S	$^2\delta(\sigma)$	1762	S	imp.
~1200	W	?	2089	S	$2^2\delta(\sigma), \nu(\pi)$
			2152	V. S.	
			2294	M	$^2\nu(\sigma)$
			3035	M	CD_2HBr+imp.
			3350	W	$^2\nu(\sigma)+{}^2\delta(\sigma)$

Spectral evidence showed the presence of an identical impurity in CD_3Cl and CD_3Br. In the case of CD_3Cl it was possible to remove the impurity by absorbing it on active charcoal at dry-ice temperature and distilling CD_3Cl off at room temperature. After this treatment the CD_3Cl did not show any of the suspected impurity bands (see Fig. 1). On heating the charcoal with the blowpipe a substance was collected in the trap of the absorption cell which gave the spectrum of the impurity. This substance has a very strong absorption even at a pressure of 5 mm Hg. In the plots of the absorption curves for CD_3Cl the absorption curve of the impurity and the pure CD_3Cl are given with the curves for the mixture of the two. The bands of the impurity at 5 mm Hg are given at reduced scale. CD_3Br could be purified in the same manner. The spectrum of the CD_3Br impurity showed the same bands as that in CD_3Cl. The separation on charcoal is not as complete as in the CD_3Cl case.

INFRA-RED ABSORPTION BANDS AND ASSIGNMENT

The bands of CD_3Cl and CD_3Br, observed at different pressures are given in Figs. 1 and 2.

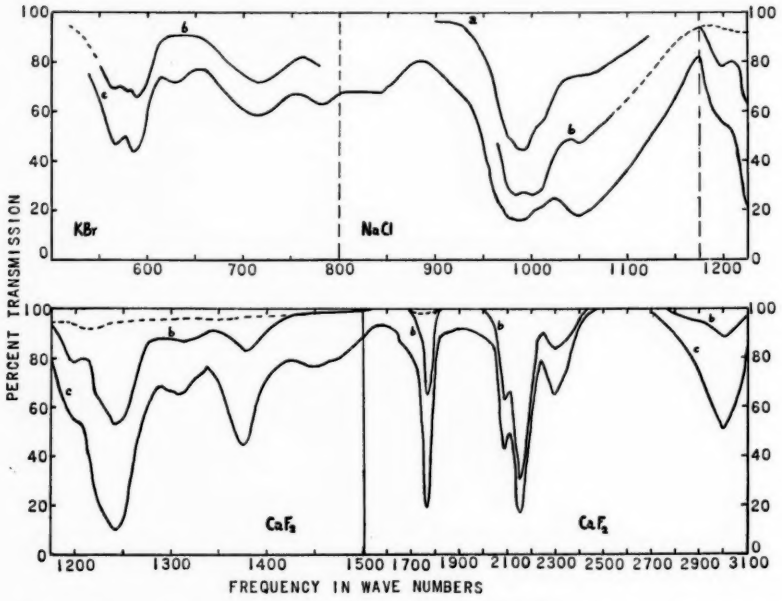

FIG. 2. Absorption spectrum of CD_3Br. Curves: (*a*) 35 mm Hg; (*b*) 89 mm Hg, – – – – – visually from records of pure CD_3Br, solid lines in 1200–1400 cm^{-1} range: CD_3Br+impurity. (*c*) 144 mm Hg.

The frequencies, their estimated intensities, and their assignments are given in Tables I and II.

Comparison of the shape and intensities of these bands with those of the ordinary methyl halides measured by Bennett and Meyer[6] leads to this assignment. We expected three parallel type bands (eventually four, if there is resonance between the first harmonic of $^2\delta(\sigma)$ and $\nu(\pi)$) and three perpendicular type bands (doubly degenerate). The intensities of these bands for the methyl halides are as follows: The higher frequency branch of $2^2\delta(\sigma)$, $\nu(\pi)$ is about twice as strong as the lower, which is about equal to $^2\nu(\sigma)$, $\delta(\pi)$ is stronger than $^2\delta(\sigma)$, $^2\tau(\sigma)$ is usually quite weak, $\nu_{C-X}(\pi)$ medium strong. This agrees with the bands observed for CD_3Cl and CD_3Br. The $P-R$ branch spacings could only be measured for two bands $\delta(\pi)$ and $\nu_{C-X}(\pi)$. They are given in Table III. The calculated values,[7] with 1.72A for C–Cl, 1.88 for C–Br, 1.09 for C–H and tetrahedral angles, compare well with the measured ones. The values for CH_3Cl and CH_3Br are from Bennett and Meyer's paper:[6]

The position of $^2\delta(\sigma)$ in CD_3Cl cannot be determined very accurately since it forms the shoulder of the very strong $\delta(\pi)$ band. There are two indirect methods of determining it quite accurately. In the methyl halides the $^2\delta(\sigma)$ band remains nearly constant, changing from 1445 cm^{-1} in CH_3I to 1476 cm^{-1} in CH_3F. Then from the $^2\delta(\sigma)$ value of CD_3Br the lower limit would be 1053 cm^{-1}. The upper limit can be obtained from a consideration of the first harmonic. The

TABLE III. Doublet spacings in the isotopic methyl chlorides and bromides.

Frequency	CH_3Cl	CD_3Cl	CH_3Br	CD_3Br
exp $\delta(\pi)$	28 cm^{-1}	27 cm^{-1}	25 cm^{-1}	21 cm^{-1}
$\nu_{C-X}(\pi)$	35 cm^{-1}	31 cm^{-1}	28 cm^{-1}	22 cm^{-1}
Mean value	31.5 cm^{-1}	29.0 cm^{-1}	26.5 cm^{-1}	21.5 cm^{-1}
Calculated	31.1 cm^{-1}	29.8 cm^{-1}	25.5 cm^{-1}	23.9 cm^{-1}

TABLE IV. The resonance frequencies $2^2\delta(\sigma)$, $\nu(\pi)$.

Frequency	CH_3Br	CD_3Br	CH_3Cl	CD_3Cl
$2^2\delta(\sigma)$, $\nu(\pi)$	2860 cm^{-1}	2089	2880	2104
	2972	2152	2967	2162
Mean value	2916	2121	2924	2133
$2^2\delta(\sigma)$	2900	2106	2920	?
Δ	+16	+15	+4	+3 to +4

[6] W. H. Bennett and C. F. Meyer, Phys. Rev. **32**, 888 (1928).
[7] S. L. Gerhard and D. M. Dennison, Phys. Rev. **43**, 197 (1933).

TABLE V. Force constants of the isotopic methyl chlorides and bromides.

Constant	Type	Chlorides	Bromides	Dimensions
f_r	C−H stretch	5.01×10^{5}	5.03×10^{5}	Dynes/cm
f_α	H−C−H bending	0.5346×10^{-11}	0.5334×10^{-11}	Dynes/radian
f_β	H−C−X bending	0.6885×10^{-11}	0.6079×10^{-11}	Dynes/radian
$f_{\beta\beta}$	H−C−X interaction	-0.0288×10^{-11}	-0.0296×10^{-11}	Dynes/radian
f_R	C−X stretch	3.368×10^{5}	2.88×10^{5}	Dynes/cm
$f_{R\beta}$	H−C−X, C−X interaction	0.607×10^{-3}	0.59×10^{-3}	Dynes/cm$^{\frac{1}{2}}$ radian$^{\frac{1}{2}}$

difference between the mean value of the two bands $2^2\delta(\sigma)$, $\nu(\pi)$ and $2^2\delta(\sigma)$ seems to be constant for CH_3Br and CD_3Br and allows us to fix the upper limit of $^2\delta(\sigma)$. From Table IV the upper limit of $^2\delta(\sigma)$ is 1065 cm^{-1}. Thus $^2\delta(\sigma)$ equal to 1058 cm^{-1} should probably be correct within our limits of error.

THEORETICAL PART

The methyl group has been assumed to have the tetrahedral shape of methane, the C−H distance[8] being 1.093A. The length of the carbon-halogen bond was assumed to be 1.72A for the C−Cl and 1.88A for the C−Br bonds, respectively.[9]

TABLE VI. Calculated and observed frequencies of CH_3Cl and CD_3Cl.

	CH_3Cl			CD_3Cl		
Freq.	Calc.	Obs.	Δ %	Calc.	Obs.	Δ %
Non-degenerate class (A_1)						
$\nu(\pi)$	2948	*ca.* 2928	+0.7	2119	*ca.* 2136	−0.8
$\delta(\pi)$	1358	1355	+0.2	1034	1029	+0.5
$\nu_{C-X}(\pi)$	730	732	−0.3	691	695	−0.6
Degenerate class (E_1)						
$^2\nu(\sigma)$	3063	3047	+0.5	2280	2287	−0.8
$^2\delta(\sigma)$	1460	1460	—	1053	1058	−0.5
$^2\tau(\sigma)$	1020	1020	—	776	775	−0.15

TABLE VII. Calculated and observed frequencies of CH_3Br and CD_3Br.

	CH_3Br			CD_3Br		
Freq.	Calc.	Obs.	Δ %	Calc.	Obs.	Δ %
Non-degenerate class (A_1)						
$\nu(\pi)$	2954	*ca.* 2932	+0.8	2123	*ca.* 2134	− 0.5
$\delta(\pi)$	1302	1305	−0.2	983	987	− 0.4
$\nu_{C-Br}(\pi)$	613	610	+0.5	576	577	− 0.2
Degenerate class (E_1)						
$^2\nu(\sigma)$	3074	3061	+0.4	2297	2294	+ 0.1
$^2\delta(\sigma)$	1452	1450	+0.1	1048	1053	− 0.5
$^2\tau(\sigma)$	953	957	−0.4	717	717	—

[8] E. F. Barker and N. Ginsburg, J. Chem. Phys. **3**, 668 (1935).

The following modified valence-force type potential function* was used for the calculation:

$$2V=f_r\sum^{3}(\Delta CH)^2+f_\alpha\sum^{3}(\Delta HCH)^2+f_\beta\sum^{3}(\Delta HCX)^2+f_{\beta\beta}\sum^{6}(\Delta HCX)(\Delta HCX)+f_R(\Delta CX)^2+f_{R\beta}\sum^{6}(\Delta CX)(\Delta HCX).$$

With six force constants, it was possible to account for the 12 frequencies of the isotopic molecules to within 1 percent. The values of the force constants do not differ much from those calculated by Linnett[10] which were based on the light molecules only. The frequencies calculated and observed are given in Tables VI and VII.

Due to resonance between $\nu(\pi)$ and $2^2\delta(\sigma)$ the exact frequency of $\nu(\pi)$ cannot be obtained in the halides, thus making it impossible to determine the necessity for an interaction constant in the C−H stretches. $\nu(\pi)$ for this calculation was found by adding Δ to the mean value of the

[9] These values are rather arbitrarily chosen from electron diffraction and spectroscopic measurements by G. B. B. M. Sutherland, Nature **140**, 239 (1937); J. Chem. Phys. **7**, 1066 (1939).

* Note: This is not the most general potential function which can be written for the methyl halides. It has been found possible to represent the frequencies of the E_1 factor by a diagonal potential function: $F_\alpha'=(f_\alpha-f_{\alpha\alpha})$; $F_\beta'=(f_\beta-f_{\beta\beta})$ and $F_r'=(f_r-f_{rr})$. The A_1 frequencies can be reproduced by a diagonal potential function with one interaction term, involving $f_{R\alpha}$ and $f_{R\beta}$. The A_1 force constants in terms of internal displacement coordinates are: $F_r=(f_r+2f_{rr})$; $F_R=f_R$; $F_\alpha=[(f_\alpha+2f_{\alpha\alpha})+(f_\beta+2f_{\beta\beta})-2(f_{\alpha\beta}+2f_{\alpha\beta'})]$ and $F_{\alpha R}=\sqrt{3}(f_{R\alpha}-f_{R\beta})$. It is found experimentally that $F_r=F_r'$ which makes $f_{rr}=0$. Since $f_{\alpha\alpha}$, $f_{\beta\beta}$, $f_{\alpha\beta}$, $f_{\alpha\beta'}$ cannot be determined separately $f_{\alpha\alpha}=f_{\alpha\beta}=f_{\alpha\beta'}=0$ has been assumed conditionally and the difference $F_\alpha-2(F_\alpha'+F_\beta')$ expressed in terms of $f_{\beta\beta}$. The same has been done in the case of $(f_{R\alpha}-f_{R\beta})$; i.e., $f_{R\alpha}$ set equal to zero. The correctness of these assumptions can only be proven by obtaining the frequencies of other isotopic compounds of different symmetry with this set of force constants and comparing with experiment.

[10] J. W. Linnett, J. Chem. Phys. **8**, 91 (1940).

two observed frequencies, Δ being the difference between this value and $2^2\delta(\sigma)$. This gave for the force constants of the C−H and C−D stretches in the degenerate and non-degenerate classes nearly the same value. It is also found that the force constant for the C−D stretch is always a little (*ca.* 0.1 unit) higher than the corresponding constant for C−H. This apparent difference is due to different anharmonicity effects for the protium and deuterium stretching vibrations. The observed and calculated product rule ratios for the isotopic methyl halides differ as predicted by O. Redlich[11] in accordance with the theory.

In conclusion I should like to thank Professor E. Bright Wilson, Jr. for suggesting the study of these molecules and for his continued interest during the course of this work.

[11] O. Redlich, J. Chem. Phys. **7**, 865 (1939).

NOVEMBER, 1942 JOURNAL OF CHEMICAL PHYSICS VOLUME 10

The Near Infra-Red Absorption Spectrum of Methyl Iodide

R. T. LAGEMANN* AND H. H. NIELSEN
Mendenhall Laboratory of Physics, The Ohio State University, Columbus, Ohio

(Received August 31, 1942)

The infra-red absorption spectrum of methyl iodide vapor has been reexamined under improved conditions at 3.3, 6.9, 8, and 11.3 microns with the result that each region reveals new detail. Near 3.36 microns some regular structure of mean separation 4.8 cm^{-1} overlaps the parallel band. The Q branches of the 6.9 mu band show a definite fine structure. The Q branch of the 8 mu band converges toward lower frequencies. In the 11.3 mu band the lines composing the Q branches converge toward higher frequencies.

INTRODUCTION

THE methyl halides have long been of interest in molecular spectroscopy. Of these, methyl iodide is of present interest, both because iodine has no known isotopes to complicate the spectrum, and because none of the parallel bands have ever been resolved. Bennett and Meyer,[1] and others[2–5] also, have located and examined the absorption bands in the near infra-red as well as their instruments permitted. In view, however, of the advances in experimental technique it was felt a reexamination was warranted. This has resulted in the finding of additional detail in each region examined as well as the revealing of several interesting convergence features.

The grating spectrometer, equipped with rocksalt foreprism, used in this work has been described in earlier publications[6] from this laboratory. While measuring the absorption, appropriate echelette gratings were rotated at intervals of five seconds of arc, and at each setting a measure of the transmitted light intensity was observed with the cell of CH_3I gas in and out of the light beam. The cells were made of cylindrical glass tubing closed off at the ends with carefully prepared rocksalt windows. The cells and gratings were maintained at about 30°C. The methyl iodide was secured from the Eastman Kodak Company.

In regions where atmospheric water vapor might obscure the absorption of the CH_3I, the air in the spectrometer case was dried by means of trays of phosphoric pentoxide. Both original and replica gratings by R. W. Wood were employed. Table I lists the gratings and spectrometer constants used for each of the regions measured.

THE 3.3-MICRON REGION

Figure 1 shows the observations near 3.3 microns plotted with ordinates in percent

* Now at Emory University.
[1] W. H. Bennett and C. F. Meyer, Phys. Rev. **32**, 888 (1928).
[2] W. W. Coblentz, Publication No. 35, Carnegie Institution of Washington, 1905, p. 61.
[3] W. W. Sleator, Phys. Rev. **38**, 147 (1931).
[4] J. G. Moorhead, Phys. Rev. **39**, 788 (1932).
[5] E. F. Barker and E. K. Plyler, J. Chem. Phys. **3**, 367 (1935).
[6] W. B. Steward and H. H. Nielsen, Phys. Rev. **47**, 828 (1935).

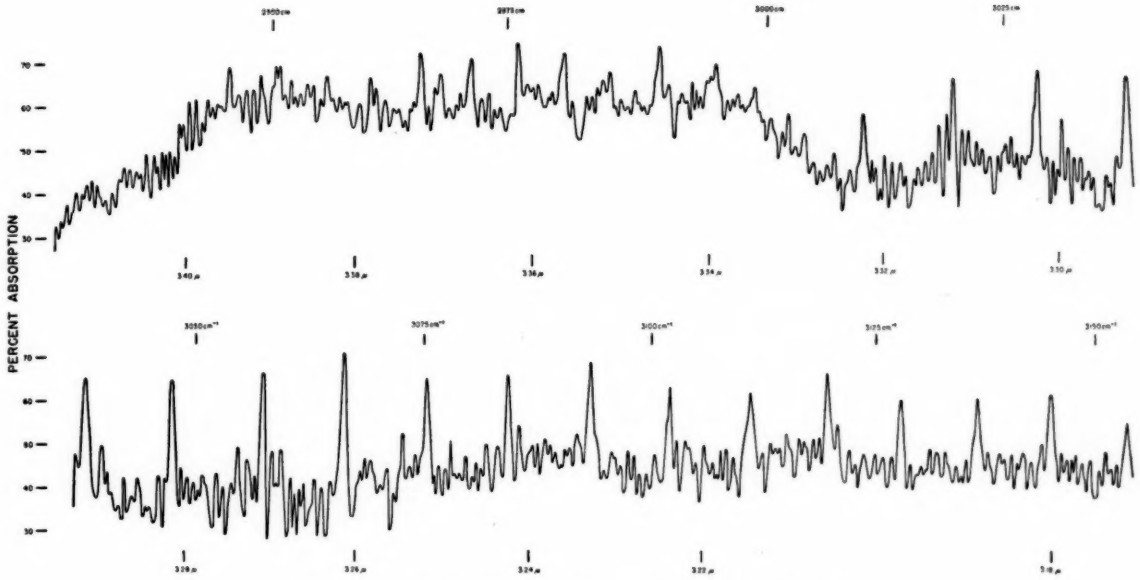

FIG. 1. The absorption of methyl iodide near 3.3 microns.

TABLE I. Experimental conditions for each of the regions of absorption.

Band (μ)	Vibration	Center (cm^{-1})	Grating (lines per inch)	Interval of reading (cm^{-1})	Effective slit width (cm^{-1})	Pressure (cm Hg)	Cell length (cm)
3.25	ν_2	3061.4	4800 original	0.23	0.45	40	11
3.3			4800 original	0.23	0.45	40	11
6.9	ν_4	1440.0	2000 original	0.12	0.48	30	10
8.0	ν_3	1251.8	2887 replica	0.06	0.18	1.3	8
11.3	ν_6	881.6	2887 replica	0.02	0.21	4	10

absorption against frequency in cm^{-1}. That part from 3.18 to 3.32 microns represents a perpendicular type of band designated as band G by Bennett and Meyer. Here the Q branches are much sharper than in the previous work, and the increased intensity of every third one is brought out more clearly. The average line separation is 8.9 cm^{-1}. Table II lists the frequency positions and separations.

TABLE II. Line frequencies and separations in the various bands.

Near 3.25μ		Near 3.36μ		Near 6.9μ		Near 11.3μ	
cm^{-1}	$\Delta\nu$	cm^{-1}	$\Delta\nu$	cm^{-1}	$\Delta\nu$	cm^{-1}	$\Delta\nu$
3010.7		2945.9		1387.2		909.2	
3020.2	9.5	2950.5	4.6	1398.9	11.7	901.0	8.2
3029.3	9.1	2955.4	4.9	1409.9	11.0	893.1	7.9
3038.5	9.2	2960.1	4.7	1422.1	12.2	885.4	7.7
3047.7	9.2	2964.9	4.8	1433.9	11.8	877.7	7.7
3056.8	9.1	2969.8	4.9	1446.0	12.1		
3065.9	9.1	2974.6	4.8	1457.8	11.8		
3075.1	9.2	2979.4	4.8	1470.0	12.2		
3084.1	9.0	2984.2	4.8	1481.3	11.3		
3093.1	9.0	2989.1	4.9	1493.1	11.8		
3102.1	9.0	2994.0	4.9	1504.8	11.7		
3111.0	8.9	2998.9	4.9	1517.8	13.0		
3119.5	8.5			1527.5	9.7		
3127.8	8.3						
3136.5	8.7						
3144.9	8.4						
3153.6	8.7						

Previous observations on the region between 3.32 and 3.41 microns indicate a parallel band ν_1. The region near 3.4 mu, which is perhaps the P branch of ν_1, indicates a spacing between rotation lines of about 0.5 cm^{-1}. This value is fairly consistent with estimates made on the value of the largest moment of inertia. Figure 1 indicates, moreover, another structure superimposed on the parallel band near 2975 cm^{-1}. This structure, which is regular, is larger in separation than one would expect for the parallel type of band. The frequency positions and separations are given in Table II. The mean separation is about 4.8 cm^{-1}. It is possible that

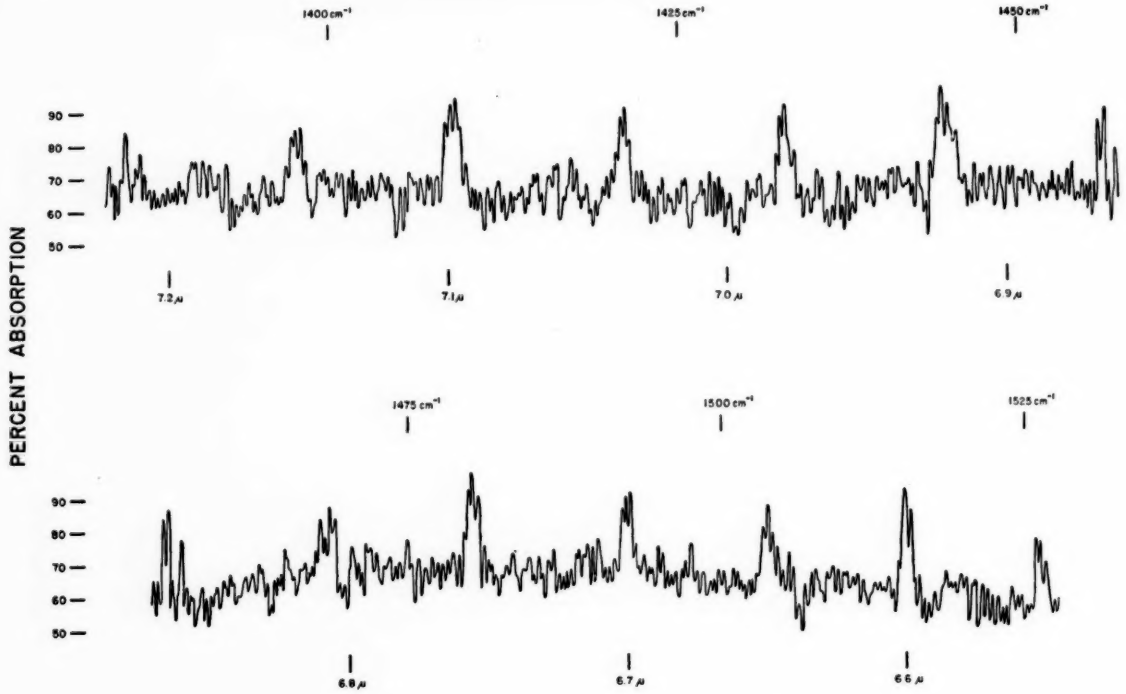

FIG. 2. The absorption of methyl iodide near 6.9 microns.

alternate lines of the superposed structure may be associated with the adjacent band, ν_2. The present work shows this region to be much weaker in absorption than indicated by Bennett and Meyer.

THE 6.9-MICRON BAND

The perpendicular band at 6.9 mu is shown in Fig. 2. It will be noted that the Q branches are not single peaks of absorption, but have been resolved into a number of components. This structure could be repeated on successive runs, although the components did not always occur with the same relative intensity. This is understandable when one considers that these details are just within the resolving power of the instrument. Table II gives the frequency positions of the centers of these Q branches. The mean separation is nearly the same as that found by Bennett and Meyer, though the present deviation from the mean is less. The P and R branch background could not be repeated with certainty. Nevertheless one run is shown.

THE 8-MICRON BAND

It was hoped at the beginning of the investigation that this band would yield a value for the moment of inertia perpendicular to the axis of symmetry. However, as can be seen from Fig. 3, the band appears quite complex, and the usual line separation cannot be measured. The lines of the Q branch appear to converge toward lower frequencies, whereas the Q branch of ν_3 of methyl chloride[7] converges toward higher frequencies.

THE 11.3-MICRON BAND

The percent absorption at 11.3 mu is shown in Fig. 4, and the frequency positions are listed in Table II. Except for the zero branches the curve is the result of only one run. It seems clear though that the lines of each zero branch converge toward higher frequencies. The maxima found by Bennett and Meyer between the zero branches are apparently not as well brought out in the present work by the gas pressure employed.

[7] A. H. Nielsen and H. H. Nielsen, Phys. Rev. **56**, 274 (1939).

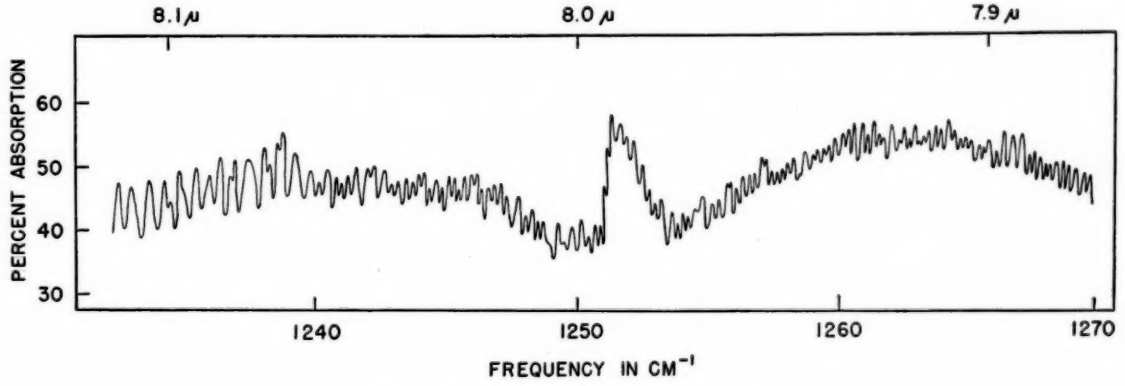

FIG. 3. The parallel band near 8 microns.

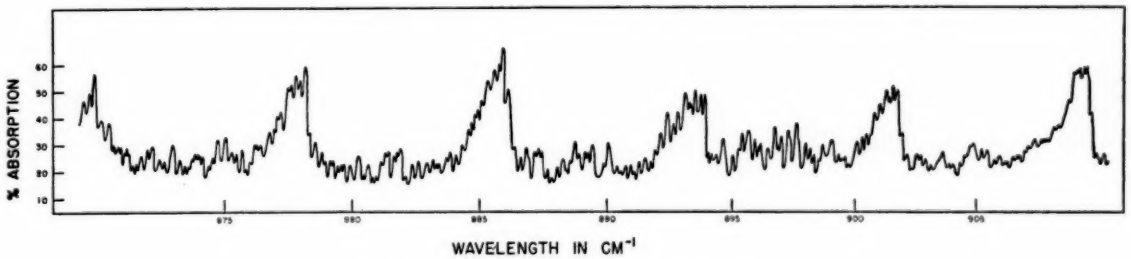

FIG. 4. The perpendicular band at 11.3 microns.

CONCLUSIONS

When listing the vibration frequencies of methyl iodide many writers use for each degenerate frequency the frequency of the strongest line at the center of the corresponding band as given by Bennett and Meyer. Since the band center really lies one-half interval toward lower frequencies from the strongest line, these frequencies have been determined and are given in the third column of Table I.

In spite of the improved resolution and dispersion used, it has not been found possible to calculate any new values for the moments of inertia and inter-nuclear distances for methyl iodide. The values given by Sutherland[8] seem consistent, however, with the results obtained. The work has revealed much of the absorption to be more complex than heretofore believed. It is expected that in the near future the spectrum will be discussed from a theoretical point of view. At that time we hope to consider the splitting of the Q branches at 6.9 mu and the various convergences noted.

[8] G. B. B. M. Sutherland, Trans. Faraday Soc. **34**, 325 (1938).

Remarks on the Absorption Spectra of Phenylalanine and Tyrosine in Connection with the Absorption in Toluene and Paracresol

H. SPONER
Department of Physics, Duke University, Durham, North Carolina

(Received August 22, 1942)

The absorption spectra of phenylalanine and tyrosine in the near ultraviolet are compared with those of toluene and paracresol and an interpretation of the individual bands is proposed.

INTRODUCTION

IT is generally recognized that the selective absorption in the near ultraviolet (2900–2400A) of the amino acids[1] phenylalanine, tyrosine, and tryptophane must be attributed to their aromatic groups. Very rough comparisons have been made between these absorptions and that of benzene, phenol, and indol, respectively, from low dispersion spectrograms.[2] If one makes use of the recent developments in the interpretation of the spectra of benzene[3] and its derivatives,[4] a better understanding of the spectra of the aromatic amino acids may be obtained.

To apply the results achieved for the benzenes we will consider phenylalanine as a toluene molecule in which one H of the CH_3 group has been substituted by the $CH(NH_2)COOH$ group. Accordingly, the tyrosine must be considered as a substituted paracresol.

The near ultraviolet absorption spectra of toluene and paracresol represent, like those of other mono- and disubstituted benzenes, allowed transitions. This means, that they have strong 0,0 bands and that the majority of bands is caused by excitation of totally symmetrical vibrations and v–v (mostly 1–1) transitions of non-totally symmetrical vibrations. If molecules are not completely unsymmetrical, there may appear in addition "forbidden" bands, that is, bands which according to electronic selection rules alone are forbidden but which appear when an unsymmetrical vibration of proper symmetry is excited with one quantum. The benzene spectrum consists only of such forbidden bands. Paracresol has no symmetry in the strict sense, hence only allowed bands will occur. Toluene has one symmetry element, namely, a plane perpendicular to the ring plane and going through one of the H atoms of the CH_3 group. Its spectrum should mainly have allowed bands and may contain some forbidden bands. It is therefore obvious, that the allowed spectrum of phenylalanine is better compared with the allowed spectrum of toluene than with the forbidden benzene spectrum.

The mentioned theoretical statements have been obtained for spectra in the vapor phase but can, with proper caution, be extended to solution spectra. Although in solutions selection rules are more likely to break down, the general appearance will be that of the gas spectrum. For example, there is no 0,0 band in the benzene vapor spectrum but it may appear weakly in solutions, while there is a strong 0,0 band in toluene in the vapor and in solution as well. But, of course, the bands are shifted in solutions with respect to the bands in the gas; also the finer structure of the vapor spectrum disappears in solutions, giving rise only to broad bands which in the vapor represent whole groups of narrower bands. Changes in polar solvents are greater than in non-polar ones.

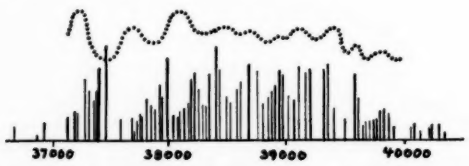

FIG. 1. Schematic representation of the absorption spectrum of toluene vapor. The curve represents the absorption in hexane solution [taken from J. Savard, Ann. de Chimie **11**, 287 (1929)].

[1] See for detailed literature references J. R. Loofbourow, Rev. Mod. Phys. **12**, 267 (1940).
[2] K. Feraud, M. S. Dunn, and J. Kaplan, J. Biol. Chem. **112**, 323 (1935).
[3] A. L. Sklar, J. Chem. Phys. **5**, 669 (1937); H. Sponer, G. Nordheim, A. L. Sklar, and E. Teller, J. Chem. Phys. **7**, 207 (1939).
[4] H. Sponer and S. H. Wollman, J. Chem. Phys. **9**, 816 (1941); I. Walerstein, Phys. Rev. **59**, 924A (1941); K. Asagoe and Y. Ikemoto, Proc. Phys. Math. Soc. Japan **22**, 677 (1940); furthermore unpublished results.

TABLE I. Comparison between spectra of toluene and phenylalanine.

Toluene vapor (ref. 5)	Assignment	Toluene in hexane (ref. 5)	Toluene in heptane (ref. 6)	Phenylalanine aqueous (ref. 2)	Phenylalanine aqueous (ref. 7)	Assignment
					36835 vw	0−600
37473 vst	0,0	37260 st	37160 st	37370	37428 w	0,0
37938 st	0+466					
37999 st	0+527	37720 m	37650 m	37825	37939 m	0+50
38401 vst	0+930	38100 st	38220 st		38361 w	0+930
38435 st	0+963	39480 vw				
38665 st	0+1193					
38929 m	0+527+930	38700 vw		38808	38838 st	0+500+900
38962 m	0+527+963					
39191 m	0+527+1193	38930 vw				
39332 m	0+2×930	39110 w				
39365 m	0+930+963					
39397 m-w	0+2×963					
39593 m	0+930+1193	39400 w	39390 st			
39628 m	0+963+1193					
		39600 w				
		39815 w		39592	39718 m	0+500+2×900
40296 w	0+2×930+963		40250 m			
40329 w	0+930+2×963					
				40605	40539 w	0+500+3×900
			41150 w	41481	41344 vw	0+500+4×900
				42540	42252 vw	0+500+5×900

COMPARISON BETWEEN TOLUENE AND PHENYLALANINE

The main results of the analyses of the spectra of toluene and phenylalanine are contained in Table I. A very rough intensity classification of the bands has been added. (vst = very strong, st = strong, m = medium, w = weak, vw = very weak.) To facilitate the understanding, the toluene spectrum has been reproduced schematically in Fig. 1. The 0,0 band at[5] 37473 is the strongest band of the first group in the spectrum and lies on the short wave-length side of that group. In solutions the group is smeared out, its maximum lying at 37260 cm^{-1} in hexane[5] and at 37160 cm^{-1} in heptane solution.[6] If our comparison is correct these broad bands correspond to one at 2671A = 37428 cm^{-1} in phenylalanine in aqueous solution.[1,7]

The next group of bands in toluene vapor consists mainly of the two strong bands 466 and 527 cm^{-1} distant from the 0,0 band towards the violet end of the spectrum. Assigning C_s symmetry to toluene the second band, at 38000 cm^{-1}, is in analogy to other substituted benzenes, best interpreted as forbidden transition made allowed by the excitation of a vibration antisymmetric to the plane defined before. This vibration corresponds to the one whose excitation (frequency value 518 cm^{-1}) is responsible for the existence of the near ultraviolet benzene spectrum. In other monosubstituted benzenes belonging to C_{2v} symmetry, the analogous vibration has a frequency of 521 in monochlorobenzene, 519 in monobromobenzene, possibly 517 in monofluorobenzene, all values referring to the excited state. In the ground state this vibration has a value of about 606–622 in all these substances because the substituent partakes only slightly in the motion. The vibration is degenerate in benzene and splits into two components in the above-mentioned monoderivatives. Besides the just discussed unsymmetrical component there is a symmetrical one of lower frequency. Although it is tempting to interpret the toluene band at 37938 cm^{-1} as caused by the excitation of this vibration the explanation is rendered doubtful because most of the strong bands have companions on the red side displaced by about 62 cm^{-1} (527 − 466 = 61).

The two discussed bands merge into one broad band in solutions. Now in phenylalanine there occurs a corresponding broad band at 2635A = 37939 cm^{-1} giving a distance of 511 from the

[5] J. Savard, Ann. de Chimie **21**, 287 (1929); there given as 37484 because the wave numbers have not been reduced to vacuum.
[6] K. L. Wolf and W. Herold, Zeits. f. physik. Chemie **B13**, 201 (1931).
[7] C. B. Coulter, F. M. Stone, and E. A. Kabat, J. Gen. Physiol. **19**, 739 (1936).

TABLE II. Comparison between the spectra of paracresol and tyrosine.

Paracresol vapor (ref. 5)	Assignment	Paracresol in hexane (ref. 5)	Paracresol in heptane (ref. 6)	Tyrosine aqueous (ref. 2)	Tyrosine aqueous (ref. 7)	Assignment
35329 vst	0,0	35000 st	35950 st	35450 st	35501 m	0,0
35748 w	0+419					
36137 vst	0+808	35750 st	36880 st	36221 st	36393 st	0+820
36516 m	0+1187	36200 st				
36944 m	0+2×808	36600 m	37450 st	37302 m	37414 w	0+1900
37323 m-w	0+1187+808	37000 m				
37752	0+3×808	37400 w	38550 m			

0,0 band. It is suggestive to assume that it represents the analogue to the above-mentioned vibrations. The only difference is that the vibration is here symmetric because phenylalanine has no symmetry element.

In this connection there should be mentioned an extremely faint band in phenylalanine[7] at 2714A = 36835 cm^{-1}. It lies 595 cm^{-1} to the red from the 0,0 band. It seems plausible to interpret it as coming from the same vibration in the lower state which has the frequency value of 511 in the upper state. From comparison with benzene and the aforementioned monosubstituted benzenes this frequency should be about 600 and indeed, a medium strong Raman line[8] has been reported at 622 cm^{-1}.

Coming back to the vapor spectrum of toluene one finds that progressions with differences[9] of 930, 962, and 1192 cm^{-1} appear superimposed on the first two groups. These differences have to be interpreted as frequencies of symmetrical vibrations in which mainly the carbon atoms of the ring are involved. The occurrence of harmonics and combination bands of these frequencies causes the groups to come closer together toward the violet end of the spectrum and therefore they appear less distinct. This will be more the case in solutions where, due to the overlapping of such groups, irregular separations may result. Thus, in heptane solution broad bands have been reported at 38220, 39390, 40250, and 41150 cm^{-1}, involving differences between 1170 and 860 cm^{-1}. In hexane solution[5] more bands have been reported, the first three being strong and distinct while the others are not.

In phenylalanine broad bands have been found by Coulter, Stone, and Kabat at 2574A = 38838 cm^{-1}, 2517A = 39718 cm^{-1}, 2466A = 40539 cm^{-1}, 2418A = 41344 cm^{-1}, and 2366A = 42252 cm^{-1}, while Feraud, Dunn, and Kaplan give for the same bands (in aqueous solution) 2576A = 38808 cm^{-1}, 2525A = 39592 cm^{-1}, 2462A = 40605 cm^{-1}, 2410A = 41481 cm^{-1}, and 2350A = 42540 cm^{-1}. Their wave-lengths have been fairly well confirmed by Anslow and Nassar.[10] These bands may be interpreted as a progression of totally symmetric vibrations (900–1000 cm^{-1}) superimposed on the transition 0+500. It seems surprising that they do not appear also as superposition on the 0,0 band. One would particularly expect a band at 0,0+about 900 because this is a strong group in toluene. Now one can see from the microphotometer tracings[7,10] that the band at 38838 is the strongest band of the spectrum; it is also quite broad so that the 0,0+900 may fall within its range. In favor of this explanation is the report of Coulter, Stone, and Kabat of a band at 2606A = 38361 cm^{-1} which appears in the right place and which evidently shows up very indistinctly. The frequencies involved in the progression correspond most probably to the strong Raman lines[8] observed at 1003 and 1032, and perhaps also to the line 1211 cm^{-1} in phenylalanine. It should be mentioned that the assignments added for the higher bands of phenylalanine contain only one possibility. It may be that in reality more vibrational transitions take

[8] N. Wright and W. C. Lee, Nature **139**, 551 (1937). Experimental condition: phenylalanine aqueous, 2 percent, 20 percent potassium iodide.

[9] The corresponding frequency values in the ground state are in all probability the strong Raman frequencies 1005, 1030, and 1212 cm^{-1}. Taken from R. Ananthakrishnan, Proc. Ind. Acad. Sci. **A3**, 52 (1936).

[10] G. A. Anslow and S. C. Nassar, J. Opt. Soc. Am. **31**, 118 (1941).

place within the range of these bands but the one in the table seems to be the most prominent.

The intensity distribution of the bands is different in toluene and phenylalanine. This is partly connected with the fact that all bands in phenylalanine represent allowed transitions while in toluene some are "forbidden" bands.

COMPARISON BETWEEN PARACRESOL AND TYROSINE

As mentioned in the introduction we shall consider tyrosine as a substituted paracresol. The general results of the analyses of the two spectra[11] are exhibited in Table II which has been arranged in the same fashion as Table I for toluene and phenylalanine. Figure 2 shows the absorption spectrum of paracresol in schematic form. Starting again with paracresol in the vapor phase, the spectrum consists chiefly of a progression of bands with separations of 808 cm^{-1} beginning with the 0,0 band at 35329 cm^{-1}. The separation belongs to a totally symmetric vibration whose value in the ground state, taken from Raman measurements,[12] is very likely 841 cm^{-1}. The first two groups (0,0 band and 0+808) of this progression are the strongest in the whole spectrum. Another group whose intensity is about the same as that of $0+2\times808$ lies about 1187 cm^{-1} (this is the position of the most intense band at 36516) to the violet from the 0,0 band. Superimposed on it appear weaker bands with the 808 separation. The 1187 belongs to another symmetric vibration with a value of 1213 or 1251 in the ground state.[12] A weak band at 35748 indicates a vibrational frequency of 419 cm^{-1} in the upper state (probably 464 in the lower state[12]). From these remarks we see that the spectrum will have the appearance of groups with rough distances from the 0,0 band of 800, 1200, 2×800, $1200+800$, 3×800, the higher members being hardly observable. This characteristic is preserved in hexane solution[5] and to a lesser degree in heptane solution where only four groups have been reported.[6]

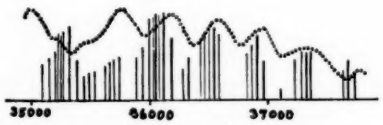

FIG. 2. Schematic representation of the absorption spectrum of paracresol vapor. The curve represents the absorption in hexane solution [taken from J. Savard, Ann. de Chimie **11**, 287 (1929)].

The fact that only three groups have been observed in the tyrosine spectrum is in favor of considering it a modified paracresol spectrum. The 0,0 band lies at 35450 cm^{-1}. The distance between the first two bands is about 820 (average value) and in all probability corresponds to the strong Raman line[13] at 844 cm^{-1}. The next group which is broader and weaker may contain two vibrational transitions, namely, 2×800 and $0+820+1100$. In fact, another strong Raman line[13] was found at 1216 cm^{-1}. All transitions involve symmetric vibrations.

We may mention that the mechanism of the production of the spectra of simple substituted benzenes seems to be preserved to a large extent not only in solution spectra of the aromatic amino acids but also in proteins containing these substances.

Finally, some remarks may be made as to the sharpness of the different spectra. The toluene spectrum in the vapor state is much sharper than that of paracresol. The latter looks as if predissociation occurs over its total range while in toluene it sets in only toward the short wavelength end of the spectrum. This predissociation is characteristic for benzene and all known derivative spectra. In benzene it has been brought in connection with the rupture of one CH bond,[14] assuming that although the vibrational energy is mostly accumulated in the totally symmetric *C*-vibration, the oscillation energy may, on account of anharmonic forces, go over into the stretching of a C−H bond. In substituted benzenes there is in addition the possibility for the rupture of other bonds involved with other repulsive curves. If the comparison used here is correct, one might expect from the appearance

[11] The interpretation of the paracresol spectrum (and also of the toluene spectrum) differs, for most bands, from the one given by Savard, but is in agreement with the recent analyses of other monoderivatives of benzene.

[12] K. W. F. Kohlrausch and A. Pongratz, Monats. f. Chem. **63**, 427 (1933).

[13] N. Wright and W. C. Lee, Nature **136**, 300 (1935). (Tyrosine, 5 percent in 0.9*N* HCl.)

[14] G. Nordheim, H. Sponer, and E. Teller, J. Chem. Phys. **8**, 455 (1940).

of the toluene and paracresol spectra that there is more tendency towards photo-decomposition in tyrosine than in phenylalanine.

The spectra of phenylalanine and of tyrosine beyond 2500A are continuous. They consist of more than one absorption system. About 2200A there is expected another absorption of the ring which corresponds to the benzene absorption at 2000A. Furthermore, the "end absorption" of all amino acids irrespective of an aromatic nucleus begins below 2500A and is attributed to the amino group. Due to overlapping it will probably not be possible to separate these different absorptions.

NOVEMBER, 1942 JOURNAL OF CHEMICAL PHYSICS VOLUME 10

The Mercury Photosensitized Reactions of Ethylene at High Temperatures*

D. J. LEROY AND E. W. R. STEACIE
National Research Laboratories, Ottawa, Canada

(Received August 10, 1942)

The mercury ($^3P_1$) photosensitized reactions of ethylene have been investigated over the temperature range 25°C to 350°C. In addition to those previously found at 25°C, the reaction $Hg(^3P_1)+C_2H_4=C_2H_3+H+Hg(^1S_0)$ is shown to occur. There was a considerable increase in the quantum yield at high temperatures and this is attributed to the hydrogen atom and vinyl radical sensitized polymerization of ethylene. The reactions of ethylene with $Na(^2P)$, $Cd(^3P_1)$, $Zn(^3P_1)$, $Hg(^3P_1)$, $Cd(^1P_1)$, and $Zn(^1P_1)$ atoms are summarized and the latter three are shown to be closely related.

INTRODUCTION

In a number of recent papers it has been established with considerable certainty that in the mercury ($^3P_1$) and cadmium ($^3P_1$) photosensitized reactions of ethane[1-3] and propane[4,5] the initial step consists in the removal of a hydrogen atom with the production of the corresponding alkyl radical. In contrast with this behavior of the paraffins, that of ethylene is much more complex. The mercury photosensitized reactions of ethylene[6] have been shown to involve the steps

$$Hg(^3P_1)+C_2H_4\rightarrow C_2H_4^*, \quad (1)$$

$$C_2H_4^*+C_2H_4\rightarrow 2C_2H_4, \quad (2)$$

$$C_2H_4^*\rightarrow C_2H_2+H_2. \quad (3)$$

On the other hand, the initial step in the cadmium ($^1P_1$)[7] and zinc ($^1P_1$)[8] photosensitized reactions of ethylene is probably the removal of a hydrogen atom with the formation of a vinyl radical, although the simultaneous occurrence of reactions analogous to those with mercury ($^3P_1$) is not excluded.

Such differences were not unexpected in view of the energies involved. The latest estimates of the C−H bond strength in ethane[9-11] are in the neighborhood of 96 to 98 kcal. while that of propane[9] is 95.5 or 91 kcal. depending on whether the H is removed from a primary or a secondary carbon atom. This makes it possible for a $Hg(^3P_1)$ atom (112.2 kcal.) to remove a hydrogen atom even if the hydride ($\Delta H=8.5$ kcal.) is not formed and for a $Cd(^3P_1)$ atom (87.3 kcal.) to remove one provided the hydride ($\Delta H=15.5$ kcal.) is formed. On the other hand, while the C−H bond strength in ethylene is not known

* Contribution No. 1079 from the National Research Laboratories, Ottawa, Canada.

[1] E. W. R. Steacie and N. W. F. Phillips, Can. J. Research **B16**, 303 (1938).

[2] E. W. R. Steacie and R. L. Cunningham, J. Chem. Phys. **8**, 800 (1940).

[3] E. W. R. Steacie and R. Potvin, J. Chem. Phys. **7**, 782 (1939).

[4] E. W. R. Steacie and D. J. Dewar, J. Chem. Phys. **8**, 571 (1940).

[5] E. W. R. Steacie, D. J. LeRoy, and R. Potvin, J. Chem. Phys. **9**, 306 (1941).

[6] D. J. LeRoy and E. W. R. Steacie, J. Chem. Phys. **9**, 829 (1941).

[7] E. W. R. Steacie and D. J. LeRoy, J. Chem. Phys. **10**, 22 (1942).

[8] H. Habeeb, D. J. LeRoy, and E. W. R. Steacie, J. Chem. Phys. **10**, 261 (1942).

[9] E. C. Baughan, M. G. Evans, and M. Polanyi, Trans. Faraday Soc. **37**, 377 (1941).

[10] D. P. Stevenson, J. Chem. Phys. **10**, 291 (1942).

[11] H. G. Andersen, G. B. Kistiakowsky, and E. R. Van Artsdalen, J. Chem. Phys. **10**, 305 (1942).

with any certainty, it is probably somewhat greater than that in ethane. The fact that neither $Cd(^3P_1)$ nor $Zn(^3P_1)$ atoms (92.5 kcal.) are able to break the C−H bond in ethylene efficiently and that reaction between ethylene and $Hg(^3P_1)$ atoms is largely (1)–(3) while that with $Cd(^1P_1)$ atoms is probably

$$Cd(^1P_1)+C_2H_4\rightarrow C_2H_3+H+Cd \text{ (or CdH)},$$

seems to indicate that the C−H bond strength is between 112.2 and 139.9 kcal. There is one difference, however, in the latter two cases. The mercury reaction was investigated at 25°C while the cadmium as well as the zinc reactions were done in the neighborhood of 300°C. This fact led us to the decision to investigate the mercury reaction over a range of temperatures and as we will show below the results more than justified the effort.

EXPERIMENTAL PROCEDURE

Two different types of apparatus were used, the first in which accurate pressure readings were taken and the second in which the products were investigated.

In the first case the reaction vessel consisted of a fused quartz annular cell 12 cm long, 9 cm in diameter with a 5.5-cm diameter hole through the middle. It was mounted in the center of a tubular furnace 90 cm long and 30-cm external diameter. The lamp was inserted through the middle of the cell. A quartz window 3 cm in diameter in the center of the furnace made it possible to examine the lamp without removing it from the furnace. A small trap containing mercury was connected to each end of the reaction vessel just outside the furnace. The mercury in the traps was maintained at room temperature. The gas was kept saturated with mercury vapor by passing it back and forth over the mercury surface in these traps. This was done by raising and lowering two small bulbs containing mercury. Since the bulbs were joined at the bottom the volume of the system was kept constant thus permitting accurate pressure readings to be made during a run. The pressures were read on a wide bore U-tube manometer using the same technique described previously.[6] The total volume of this system was approximately 670 cc, most of which was in the furnace.

In order to make certain that no $Hg(^1P_1)$ atoms were present due to the fused quartz transmitting 1849A, a few runs were made with a thin Pyrex filter between the lamp and reaction vessel. A Pyrex tube approximately 30-mm O.D. was thickened over a distance of a few mm and drawn out and blown simultaneously resulting in a thin portion about 30 mm long and of approximately the same diameter as the rest of the tube. Since the transmission of 2537A was cut down by a factor of approximately 30 it is highly improbable that any light of wave-length 1849A was transmitted.

In the other static runs the light intensity was cut down by a factor of about 20 by inserting a slotted brass tube between the lamp and reaction vessel. The slots extended half way around the diameter of the tube and alternated on the different sides. The number of slots per inch was varied till a suitable rate of pressure change was obtained, permitting accurate readings spread over about three quarters of an hour.

The lamp was of the low pressure type used previously and consisted of a straight tube 100 cm long with an electrode chamber on each end. The central part was of quartz with graded seals connecting to Pyrex. The over-all length was 120 cm, thus permitting the electrode chambers to be outside the furnace. To keep the mercury vapor pressure in the lamp at approximately 2×10^{-3} mm a short tube fastened to the main tube projected downwards and contained mercury. This tube was always kept at room temperature. Tests made with an F.J. 405 photo-tube showed that the light intensity was practically the same at 300°C as at 25°C.

In the apparatus used to determine products, the lamp, reaction vessel, and furnace were the same as that described above with the exception that the slotted brass tube was removed and the full radiation of the lamp used. The remainder of the apparatus was the same as the circulating system described previously.[6] The total volume of this system was approximately 3500 cc. The non-condensible gas was isolated by passing the products through a trap cooled to approximately −200°C. This temperature was obtained by pumping down the liquid air in the vacuum flask surrounding the trap by means of a Hyvac. The volume of non-condensible gas was measured by

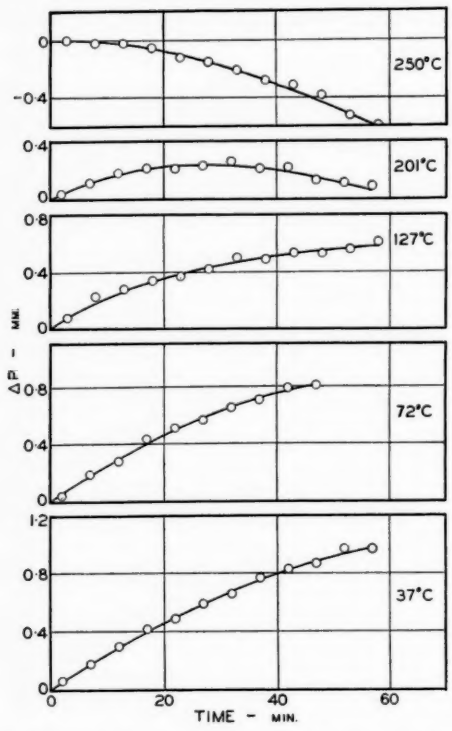

FIG. 1. Pressure change *vs.* time. Initial pressure 15 mm.

compressing it into a calibrated volume by means of a small mercury diffusion pump backed by a Toepler pump. The method of analysis of this gas as well as that of the other products has already been described.[6] The non-condensible gas was found to be entirely hydrogen.

The ethylene used in these experiments was purified in the same manner as before. Nitric oxide was prepared by the reaction of mercury on a two percent solution of sodium nitrite in concentrated sulphuric acid. It was passed through a trap containing a dry ice-acetone mixture and further purified by a bulb-to-bulb distillation using liquid air. Since it was found that ethylene-nitric oxide mixtures reacted slowly at room temperatures forming a deposit on the walls of the storage vessel, these mixtures were made up immediately before they were used.

RESULTS

In Fig. 1 the pressure changes for a series of runs at 15-mm pressure are shown. These results are in sharp contrast to Melville's statement[12] that temperature has no effect on the reaction. The initial rate of pressure increase decreases as the temperature is raised till at 250°C the initial pressure rise has disappeared altogether. The possibility that this difference might be due to some $Hg(^1P_1)$ atoms being present was discounted when it was found that runs in which the thin Pyrex filter was used showed the same effect. Furthermore, the relative rates at 25°C and at 300°C were the same with the Pyrex filter as with the slotted brass tube.

In our previous investigation at 25°C it was found that in the early stages the rate of disappearance of ethylene decreased as the pressure was increased. This was closely tied up with the rate of formation of acetylene and hydrogen as expressed in Eqs. (1)–(3). At higher temperatures, on the other hand, it was found that the rate of pressure decrease was greater at higher pressures. This is shown in Fig. 2.

That the effect of pressure on the rate of production of acetylene and hydrogen is not greatly different at high temperatures is shown in Figs. 3 and 4. Although the rate of production of both acetylene and hydrogen is greater at 300°C than at 25°C, it is seen that in both cases an increase in pressure results in a decrease in the rate of production of these products. At both

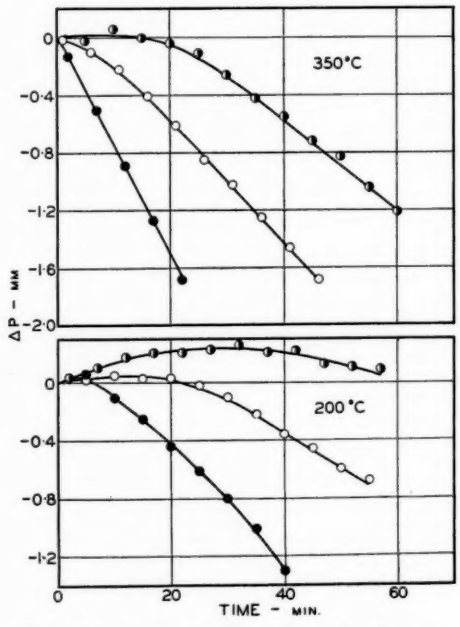

FIG. 2. Pressure change *vs.* time. ◑, 15 mm; ○, 30 mm; ●, 70 mm.

[12] H. W. Melville, Trans. Faraday Soc. **32**, 258 (1936).

100-mm and 400-mm pressure the rate is greater at 300°C than at 25°C. The reason for this is clear when we realize that for a given pressure the number of deactivating collisions per second is less at 300°C than at 25°C. In other words, the rate of reaction (3) relative to that of (2) is greater at the higher temperature.

Figures 3 and 4 also show that at 300°C the rate of formation of hydrogen is greater than that of acetylene. This could be due to a number of causes. It must be remembered that in contrast to 25°C, the pressure is decreasing quite rapidly due to the formation of substances other than hydrogen and acetylene and there is always a possibility that hydrogen may be formed by secondary reactions. Another possibility is that acetylene may not be as inert at 300°C as it was at 25°C and that it may form a co-polymer with ethylene, for example.[13]

EFFECT OF NITRIC OXIDE ON THE REACTION

If, as seems to be the case, free radicals are formed in the initial stages of the reaction at high temperatures and reactions of these radicals are responsible for the rapid pressure decrease, then it is possible that polymerization might be inhibited by the presence of nitric oxide. Figure 5 shows the pressure changes in a series of runs at 15 mm-pressure and 300°C using various percentages of nitric oxide, namely, 0, 3 percent, 10 percent, and 19 percent. These curves have been shifted vertically by 0.5 mm to avoid congestion. In the presence of 10 percent or more of nitric oxide the initial rate of pressure *increase* is practically identical with that at 25°C with no nitric oxide present (Fig. 6). That nitric oxide has little or no effect on the initial rate of pressure increase at 25°C is also shown in Fig. 6 where the pressure changes for a 14.7 percent mixture are given. It does, however, affect the height of the maximum, since at this pressure the maximum pressure increase is about 1.5 mm at 25°C.[6]

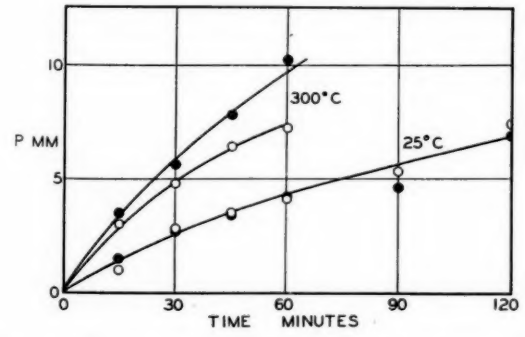

FIG. 3. Pressure of hydrogen and acetylene *vs.* time. ●, hydrogen; ○, acetylene. Initial pressure 100 mm.

[13] Naragon, Burk, and Lankelma, Ind. Eng. Chem. **34**, 355 (1942).

Products

A comparison of the products formed at 25°C and at 300°C is shown in Table I. The time is given in minutes. The volume of higher products is in cc of liquid, that of the other products in cc of gas at 25°C and 760 mm. Hydrogen was removed and measured as previously described. Ethylene and acetylene were distilled off and acetylene determined in the mixture. In order to get enough products for a distillation, four runs were made at 25°C and the products (other than ethylene, acetylene, and hydrogen) combined.

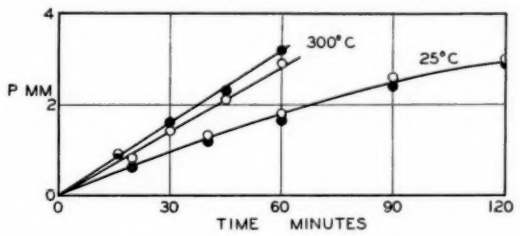

FIG. 4. Pressure of hydrogen and acetylene *vs.* time. ●, hydrogen; ○, acetylene; ◒, overlapping points. Initial pressure 400 mm.

The most interesting thing about these runs is that propylene is formed in relatively large amounts at 300°C, although none was found at room temperature. Furthermore, as might be expected, for the same yield of acetylene the production of "higher liquids" is greatly increased.

An idea of the amount of ethylene used up in processes other than the production of hydrogen and acetylene is obtained from the data in Table II. This table gives further information on the runs shown in Figs. 3 and 4. The initial pressure p and the pressure increase Δp are in mm. V_0 is the original volume of ethylene, V_{cond} is the volume of gas condensible in liquid air at the end of the run, and $V_{C_2H_2}$ is the volume of

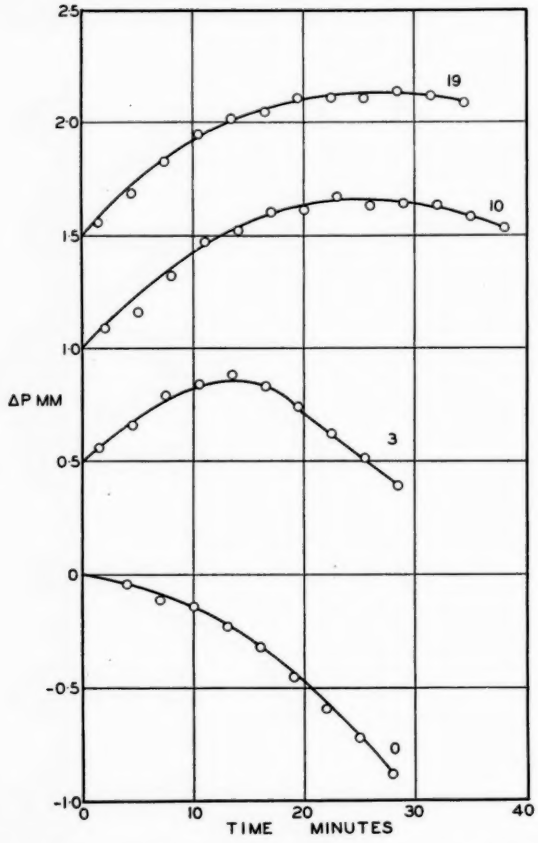

FIG. 5. Pressure change *vs.* time in the presence of nitric oxide. Initial pressure 15 mm, 300°C.

acetylene produced, all in cc at 25°C and 760 mm. If the average molecular weight of the products is high, the volume of ethylene used up by processes other than the production of hydrogen and acetylene is given by $V_0 - V_{cond}$. If the average molecular weight corresponded to C_4 it would be twice this. While the accuracy of such measurements is not high it is clear that the quantum yield of ethylene disappearance by these other processes is greater at 300°C than at 25°C by a factor of five to ten.

DISCUSSION

As we have mentioned above, there appears to be little doubt that the reactions leading to the formation of hydrogen and acetylene are not changed on raising the temperature. That is to say, their rate of production is determined by reactions (1), (2), and (3). Whether hydrogen is produced by reactions other than (3) or whether acetylene is used up is not certain although it appears from Fig. 3 that the latter is more probable. In the reaction of $Cd(^1P_1)$ atoms with ethylene[7] it was found that acetylene formation dropped off as a run progressed till it reached a constant value. Further comparison shows that in both cases the ratio of pressure decrease to acetylene formation increased with increasing pressure, the actual ratios being of the same order of magnitude for $Hg(^3P_1)$ and $Cd(^1P_1)$ atoms under similar conditions of temperature.

In our discussion of the reaction of $Cd(^1P_1)$ atoms with ethylene[7] we were forced to the conclusion that reactions of the type (1)–(3) alone could not account for the results even in the early stages of the reaction. The complete absence of any initial pressure rise indicated that primary processes other than those corresponding to (1)–(3) must occur. If the pressure decrease were due solely to the onset of the hydrogen atom sensitized polymerization of ethylene, as found in the later stages of the $Hg(^3P_1)$ reaction at room temperature, and if the only process leading to the formation of hydrogen atoms were the reaction

$$M^* + H_2 \rightarrow 2H + M, \qquad (4)$$

then the initial pressure decrease could not be explained. Even a large increase in the quantum yield of the hydrogen atom sensitized polymerization of ethylene would not eliminate at least a small pressure increase until the concentration of molecular hydrogen was sufficient to permit it quenching the $Cd(^1P_1)$ or $Cd(^3P_1)$ atoms.

Similar considerations to those above apply to the $Hg(^3P_1)$ reaction at high temperatures. Just as we were forced to assume the reaction

$$Cd(^1P_1) + C_2H_4 \rightarrow C_2H_3 + CdH, \qquad (5)$$

so we believe that the high temperature results with $Hg(^3P_1)$ atoms can be accounted for on the

TABLE I. Initial pressure = 150 mm.

No.	Temp.	Time	C_2H_2	H_2	C_3H_6	C_4	Higher
179	300	180	22.3	33.6	50.5	13.5	0.21
180	300	229	24.2	38.2	49.0	18.0	0.26
172	25	247	28.0	39.0			
173	25	239	22.9	37.4	0	37.0	0.09
174	25	248	20.1	34.2			
175	25	243	19.7	32.2			

assumption that the reaction

$$Hg(^3P_1)+C_2H_4\rightarrow C_2H_3+H+Hg(^1S_0) \quad (6)$$

or

$$Hg(^3P_1)+C_2H_4\rightarrow C_2H_3+HgH \quad (7)$$

takes place. At 25°C the early stages of the reaction were accounted for quantitatively by reactions (1)–(3). However, we mentioned that at higher pressures there was evidence of polymerization occurring by some other process. This effect is further brought out in our present work. In Table II it can be seen that at 25°C there was some ethylene disappearing by reactions other than the formation of hydrogen and acetylene even when the concentration of molecular hydrogen was small.

Polymerization of ethylene sensitized by hydrogen atoms and vinyl radicals would be expected to be more rapid at high pressures.

It is quite possible, then, that reaction (6) or (7) did occur at 25°C, although to a much smaller extent than reactions (1), (2), and (3). The number of $Hg(^3P_1)$ atoms leading to reactions (6) or (7) must be relatively small since the quantum yield at 25°C and 13 mm was 0.37 and if we allow for loss of $Hg(^3P_1)$ atoms by reaction (1) followed by (2) it is clear that the number available for reactions (6) or (7) cannot be very large.

There are two possible ways of explaining the increase in quantum yield and the absence of an initial pressure rise at high temperatures: (1) We can assume that the number of $Hg(^3P_1)$ atoms used up in reactions (6) or (7) is increased or (2) the quantum yield of the hydrogen atom and vinyl radical sensitized polymerization of ethylene is higher at high temperatures. The latter seems the more likely since the production of hydrogen and acetylene appears to be independent of temperature. In either case polymerization would be inhibited by nitric oxide.

TABLE II.

No.	Temp.	p	Time	Δp	V_0	V_{cond}	$V_{C_2H_2}$	V_0-V_{cond}
201	300	400	16	-17.0	185_0	178_3	4.1	6_7
202	300	400	30	-28.3	183_0	169_9	6.4	13_1
204	300	400	45	-37.7	186_5	168_0	9.8	18_5
203	300	400	60	-50.0	185_0	158_8	13.5	26_2
206	300	100	15	-7.0	46_0	41_2	13.9	4_8
207	300	100	30	-12.5	46_0	37_4	22.0	8_6
209	300	100	45	-19.5	46_0	33_2	29.4	12_8
208	300	100	64	-27.5	46_0	28_9	33.0	17_1
216	25	400	20	$+0.5$	197_5	196_2	3.9	1_3
217	25	400	40	-1.5	197_5	195_0	6.4	2_5
218	25	400	60	-1.0	198_0	195_0	8.7	3_0
219	25	400	90	-1.0	197_2	194_2	12.9	3_0
220	25	400	120	-2.0	196_0	190_8	14.8	5_2
210	25	100	15	0.0	49_5	48_2	4.8	1_3
211	25	100	30	$+1.0$	49_4	48_2	13.8	1_2
213	25	100	45	$+1.0$	49_7	47_4	17.4	2_3
214	25	100	60	$+1.0$	49_4	46_7	20.2	2_7
215	25	100	90	$+1.0$	49_4	46_8	26.2	2_6
212	25	100	120	0.0	49_4	44_8	36.6	4_6

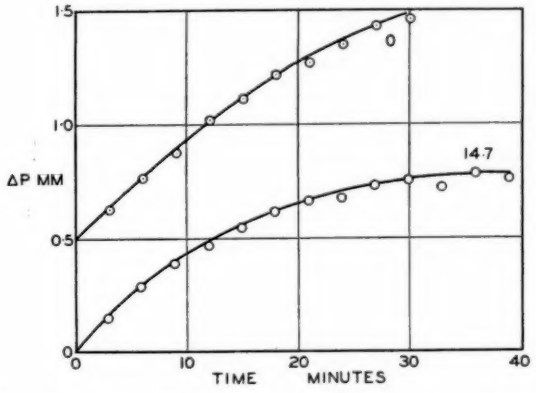

FIG. 6. Pressure change *vs.* time in the presence of nitric oxide. Initial pressure 15 mm, 25°C.

No direct evidence has ever been found for the existence of the vinyl radical, although Eltenton[14] was able to detect the allyl radical in the reaction of methyl radicals with propylene. He attributed his inability to detect the vinyl radical to its high reactivity. One would not expect to find any appreciable quantity of products with the empirical formula, C_nH_{2n-2} (other than acetylene). The large quantum yield of the sensitized polymerization of ethylene coupled with the fact that only one diene molecule would be found for each vinyl radical produced in reactions (6) or (7) would make it practically impossible to detect such compounds.

We can then assume that the large quantum yield at high temperatures is due to reactions of the type

$$C_2H_3+C_2H_4\rightarrow C_4H_7,$$
$$C_4H_7+C_2H_4\rightarrow C_6H_{11}, \text{ etc.},$$

and

$$H+C_2H_4\rightarrow C_2H_5,$$
$$C_2H_5+C_2H_4\rightarrow C_4H_9, \text{ etc.},$$

[14] G. C. Eltenton, J. Chem. Phys. **10**, 403 (1942).

TABLE III.

Sensitizer	Wavelength	Excitation energy	Heat of formation of hydride	Quenching cross section	Remarks
$Na(^2P)$	5890 5896	48.3	51.6	44.0[a]	No reaction[b]
$Cd(^3P_1)$	3261	87.3	15.5	26.5[c]	Slow reaction
$Zn(^3P_1)$	3076	92.5	23.1	?	Slow reaction
$Hg(^3P_1)$	2537	112.2	8.5	48.0[d]	Fast reaction
$Cd(^1P_1)$	2288	124.4	15.5	High "absorption"	Fast reaction
$Zn(^1P_1)$	2139	133.4	23.1	High "absorption"	Fast reaction

[a] R. G. W. Norrish and W. MacF. Smith, Proc. Roy. Soc. **A176**, 295 (1940).
[b] J. C. Jungers and H. S. Taylor, J. Chem. Phys. **4**, 94 (1936).
[c] E. W. R. Steacie and D. J. LeRoy, unpublished.
[d] E. W. R. Steacie, Can. J. Research **B18**, 44 (1940).

together with chain transfer and the usual chain stopping steps of radical recombination and decomposition. The formation of propylene at high temperatures is probably the result of the decomposition of butyl radicals by the reaction

$$C_4H_9 \rightarrow C_3H_6 + CH_3.$$

This would be more important at 300°C than at 25°C and would tend to increase the quantum yield due to the methyl radical sensitized polymerization of ethylene.

In this connection it is interesting to note that in the $Zn(^1P_1)$ photosensitized reactions of ethylene, propylene was one of the most important products. It was not formed in very large amounts in the $Cd(^1P_1)$ reactions, however, a fact which does not have any immediate explanation.

Apart from this one fact, the present investigation brings all the work on the photosensitized polymerizations of ethylene into line. These investigations are summarized in Table III. Where quenching data are known they are given in A². A "slow" reaction indicates that the quantum yield is of the order 0.01 to 0.05. Energies are in kcal.

It will be seen that the reaction with $Na(^2P)$, $Cd(^3P_1)$, and $Zn(^3P_1)$ atoms is very slow in spite of the large quenching cross sections, the energies apparently being too small. On the other hand, the reaction with $Hg(^3P_1)$, $Cd(^1P_1)$, and $Zn(^1P_1)$ atoms is quite rapid. Furthermore, the mechanism for these latter reactions now appears to be identical for the three cases, namely,

$$M^* + C_2H_4 \rightarrow C_2H_3 + H + M$$

or

$$\rightarrow C_2H_3 + MH,$$

followed by an H atom and vinyl radical sensitized polymerization of ethylene.

In addition, acetylene is probably formed in all cases by the over-all process

$$M^* + C_2H_4 \rightarrow C_2H_2 + H_2 + M.$$

It should, of course, be emphasized that relating excitation energies to bond strengths is a drastic approximation. Any precise treatment of the transfer of energy from a sensitizer to a reactant must involve a detailed consideration of the transition states.[15] However, the fact that the reactions of $Hg(^3P_1)$ atoms fall in with those of the high energy group, in spite of the difference in multiplicity, indicates that the approximation of a simple transfer of energy is not inconsistent with the data on ethylene.

The authors would like to express their indebtedness to Mr. A. VanWinckel for assistance in carrying out the experiments.

[15] K. J. Laidler, J. Chem. Phys. **10**, 34, 43 (1942).

The Cadmium ($^3P_1$) Photosensitized Reactions of the Lower Olefins*

D. J. LeRoy and E. W. R. Steacie
National Research Laboratories, Ottawa, Canada

(Received September 3, 1942)

An investigation has been made of the cadmium ($^3P_1$) photosensitized reactions of ethylene, propylene, butene-1, and butene-2. The low quantum yields are attributed to the influence of the C=C bond on the actual quenching process and are not inconsistent with the data on C–H bond strengths.

SEVERAL investigations have been made on the reactions of the lower paraffins with $Hg(^3P_1)$ and $Cd(^3P_1)$ atoms.[1] In every case the primary step was found to be

$$M^*+R-H=R+H+M \text{ (or MH)}. \quad (1)$$

On the other hand the olefins react somewhat differently. The reaction of $Hg(^3P_1)$ atoms with ethylene involved the steps

$$Hg(^3P_1)+C_2H_4=C_2H_4^*+Hg(^1S_0), \quad (2)$$

$$C_2H_4^*+C_2H_4=2C_2H_4, \quad (3)$$

$$C_2H_4^*=C_2H_2+H_2, \quad (4)$$

as well as the reaction corresponding to (1). $Cd(^1P_1)$ and $Zn(^1P_1)$ atoms appeared to react in the same way, the importance of (1) relative to (2), (3), and (4) decreasing in the order $Zn(^1P_1)>Cd(^1P_1)>Hg(^3P_1)$. The reaction with $Cd(^3P_1)$ atoms was found to have a very low quantum yield (*ca.* 0.01).[2] These reactions have been discussed in relation to the corresponding excitation energies.[1]

The difference between the paraffins and ethylene would seem to be closely connected with the presence of the C=C bond in the latter as compared to the C–C bonds in the paraffins, and the effect of these bonds on the C–H bond strength. The problem then presented itself of investigating the reactions of hydrocarbons having C–C as well as C=C bonds, namely, the other olefins. With this in mind a series of runs was made using $Cd(^3P_1)$ atoms with propylene, butene-1, and butene-2, as well as ethylene.

In every case reaction was found to be slow, so most of the measurements were made in a static system similar to that described previously.[3] For this purpose cadmium turnings were placed directly in the cell. The apparent volume of this system was 558 cc. Some runs were made in a circulating system in an attempt to collect products.

The results of the static runs are shown in Fig. 1. In every case the initial pressure was 225±2 mm. The runs were made in the order △, ◓, □, ◑, ●, ○, so the variations in rate cannot be attributed to a progressive decrease in light intensity. As shown by the curves, the rates are in the order ethylene >propylene> butene-1>butene-2.

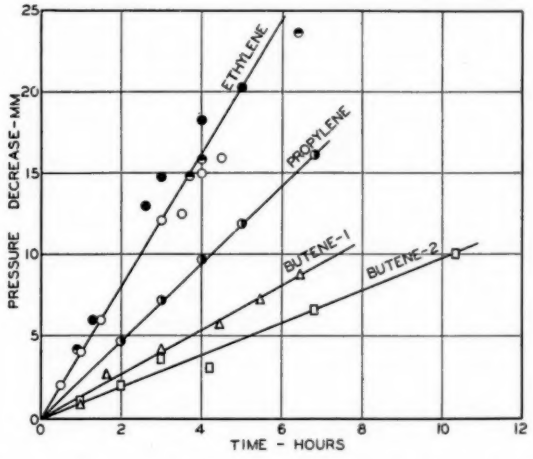

FIG. 1. Pressure decrease *vs.* time for the four olefins. Initial pressure 225±2 mm.

PRODUCTS

In view of the small amount of reaction a complete analysis of the products offered con-

* Contribution No. 1083 from the National Research Laboratories, Ottawa, Canada.

[1] See D. J. LeRoy and E. W. R. Steacie, J. Chem. Phys. 10, 676 (1942) for a summary of these reactions as well as those of $Na(^2P)$, $Hg(^3P_1)$, $Cd(^3P_1)$, $Cd(^1P_1)$, $Zn(^3P_1)$ and $Zn(^1P_1)$ atoms with ethylene.

[2] E. W. R. Steacie and R. Potvin, Can. J. Research B18, 47 (1940).

[3] E. W. R. Steacie and D. J. LeRoy, J. Chem. Phys. 10, 22 (1942).

siderable difficulty. However a limited amount of significant data was obtained.

(a) Ethylene

One run was made in which acetylene was measured. It was found to be present to the extent of 0.16 percent, but since the pressure decrease for the same run was 8.8 percent the reaction leading to acetylene formation must be of small importance compared to that leading to polymerization. No measurable quantity of non-condensable gas (hydrogen or methane) was found.

(b) Propylene

No non-condensable gas was found in a 7½-hour run in the circulating system, and the entire sample distilled as propylene, although cyclopropane or propane could have been detected if present.

(c) Butene-1

A 23-hour run was made in the circulating system. The initial pressure was 335 mm and the final pressure was 287 mm. No non-condensable gas was found and only 26 cc of gas were distilled over before the temperature reached that of boiling butene-1. Most of this was probably butene. There were 573 cc of gas distilling in the butene-1 range and approximately 45 cc in the trans-butene-2 range. There remained a residue of higher boiling liquid which was not distilled. The indication of butene-2 may or may not be significant.

(d) Butene-2

This reaction was even slower than that of butene-1. A 21½-hour run was made in the circulating system using an initial pressure of 327 mm. The pressure decrease was only about 6 mm. Approximately 4 cc of non-condensable gas were found, which is not very significant since a small amount of air may have leaked in during the transfer of the gas to the still. No other gas of smaller molecular weight than butene was found; consequently it is not surprising, in view of the small pressure change, that no appreciable amount of higher boiling liquid was found.

The most striking result of this investigation is the slow rates observed for propylene and the two butenes. As mentioned before, the initial step in the reaction of $Cd(^3P_1)$ atoms with the paraffins is the breaking of the C−H bond with the formation of CdH and the corresponding alkyl radical. Taylor and Smith[4] found a very low activation energy (3.1 kcal.) for the reaction of methyl radicals with propylene and attributed it to a low C−H bond strength on the carbon remote from the double bond. They suggested that the strength of this bond was about 5 kcal. less than that in ethane. Since recent estimates of the C−H bond strength in ethane are in the range 96 to 98 kcal.,[5–7] this would place the corresponding value for propylene in the range 91 to 93 kcal., a value close to that of the weakest C−H bond in propane.[5] Consequently one would expect that the reaction

$$Cd(^3P_1)+C_3H_6=C_3H_5+CdH \qquad (5)$$

would take place readily. Similar considerations should obtain for butene-1 and butene-2.

It is known that the reaction

$$H+C_3H_6=C_3H_7 \qquad (6)$$

takes place readily,[8] leading to the formation of hexane and propane, together with smaller amounts of methane, ethane, butane, and pentane. Also Taylor and Smith[4] found considerable polymerization of propylene which they stated

TABLE I.

Olefin	Quenching efficiency	Paraffin	Quenching efficiency
C_2H_4	26.3 mm^{-1}	C_2H_6	*ca.* 0.04 mm^{-1}
C_3H_6	26.5	C_3H_8	
C_4H_8-1	29.0	*n*-C_4H_{10}	
C_4H_8-2	25.0	*iso*-C_4H_{10}	

may be due to the sensitized polymerization of propylene by the allyl radical. At any rate one would expect that if reaction (5) did occur it

[4] H. S. Taylor and J. O. Smith, J. Chem. Phys. **8**, 543 (1940).
[5] E. C. Baughan, M. G. Evans, and M. Polanyi, Trans. Faraday Soc. **37**, 377 (1941).
[6] D. P. Stevenson, J. Chem. Phys. **10**, 291 (1942).
[7] H. G. Andersen, G. B. Kistiakowsky, and E. R. Van Artsdalen, J. Chem. Phys. **10**, 305 (1942).
[8] W. J. Moore and H. S. Taylor, J. Chem. Phys. **8**, 504 (1940).

would lead to a relatively rapid polymerization. Since this is not the case the efficiency of reaction (5) must be quite low. We must then attribute the low rate to the influence of the C=C bond on the actual quenching process rather than to the strength of the C−H bond.

The quenching efficiencies of propylene, butene-1, and butene-2 are in the same range as that of ethylene so we cannot attribute the slow reaction to this cause. Table I gives the quenching efficiencies of the four olefins together with the corresponding values for the lower paraffins.[9] These values are given by the slope of the curve obtained by plotting the reciprocal of the actual quenching against the pressure.[10]

It would appear from this table that the actual quenching process is responsible for the inefficiency of the ultimate reaction. The excitation energy of $Cd(^3P_1)$ atoms is such that reaction (1) cannot take place unless CdH is formed ($\Delta H = 15.5$ kcal.). Consequently if this energy is absorbed by the C=C bond, as seems to be the case, most of it will be dissipated as vibrational and rotational energy and not lead to reaction. Assuming that the quenching efficiency of a double bond is 600 times as great as that of a single bond, the probability of removing an H atom from the methyl group in propylene, for example, compared to the probability that the excitation energy will be absorbed by the olefinic part of the molecule will be of the order 1 : 600. The actual ratio may be even smaller than this due to steric effects. The small amount of reaction that does occur may be the result of the removal of an H atom from either the olefinic or the paraffinic part of the molecule, with the formation of CdH; or it may even be due to a pseudo-thermal polymerization resulting from collisions of activated olefin molecules with normal ones. In this connection it is worth noting that the temperature used in these experiments (285°C) is not far from the lower limit where thermal reaction begins.

The fact that $Hg(^3P_1)$ atoms react readily with ethylene to form activated ethylene molecules capable of dissociating into acetylene and hydrogen, while very little acetylene is formed with $Cd(^3P_1)$ atoms is probably due simply to the difference in excitation energy.[11] What little acetylene is formed is probably the result of reactions analogous to (2), (3), and (4).

In view of the above remarks our results are not inconsistent with those of Taylor and Smith[4] in as much as collisions of methyl radicals with propylene involve processes of quite a different character.

[9] E. W. R. Steacie and D. J. LeRoy, unpublished.

[10] A. C. G. Mitchell and M. W. Zemansky, *Resonance Radiation and Excited Atoms* (Cambridge, 1934).

[11] E. W. R. Steacie, Ann. New York Acad. Sci. **41**, 187 (1941).

Premelting Anomalies of Some Long Chain Normal Paraffin Hydrocarbons

ANDREW VAN HOOK† AND L. SILVER*
Department of Chemistry and Chemical Engineering, University of Idaho, Moscow, Idaho
(Received July 24, 1942)

The coefficients of thermal expansion of tetradecane, hexadecane, octadecane, and tetracosane have been measured continuously for considerable temperature ranges on both sides of the melting points. The increase of these coefficients in the neighborhood of the melting points is suggestive of an order-disorder mechanism for the transitions. Although the effect is observed to be larger on the solid side of the transition than on the liquid, the latter is interpreted as more significant, since the presence of impurities and the open, mosaic structure of the solid contribute largely to the increase. Likely impurities are not of the Raoult type, and do not cause appreciable variations.

INTRODUCTION

THE physical properties of the long chain paraffin hydrocarbons have assumed added significance in a recent extreme disorder theory of melting (premelting);[1] and also in the cataloging of[2] such properties of these compounds. To extend the data available for such uses the coefficients of thermal expansion of a few representative hydrocarbons, over a temperature interval including the melting point, were determined. Since the relation

$$(\partial S/\partial V)_T = -[(\partial V/\partial T)_P/(\partial V/\partial P)_T] \quad (1)$$

implies a great similarity in the specific heat and thermal expansion, it should thus be possible simultaneously to confirm the anomalous specific heat results reported by Ubbelohde,[1b] and to acquire additional expansion data. This latter is desirable because the compiled data is from only a few sources, is derived uniquely from scattered density measurements, and does not include the solid range.

Although any order-disorder mechanism of melting involves a transition other than the simple first-order type,[3] and while the experimental manifestation of this transition should be possible on either side and direction of the transition, it is apparent that the behavior on the solid side will be obscured to a much greater extent than the liquid side by the presence of any kind and amount of impurity. Hence the paramount importance of the maximum purity of materials whose properties are measured in the neighborhood of a transition temperature.

EXPERIMENTAL

A. Purification

Tetradecane, hexadecane,[4] octadecane, and tetracosane of the Eastman Kodak Company were extensively purified by a sequence of repeated fractionations, fractional crystallizations from melt and solvents, and molecular distillation. The procedure was usually in the order mentioned. The solvent crystallizations were usually from five volumes of acetone. The molecular distillations were performed in a simple Hickman type still, at an operating pressure of about 10^{-4} mm. A very fine temperature cut was taken off. Further crystallizations followed the distillations. Extensive sulfuric acid treatment was not employed in this purification scheme.[5]

The fractional crystallizations were carried out with particular care. In effect, a middle portion

* From the M.S. Thesis of Mr. Silver, University of Idaho, 1942.

† Present address: Chemistry Department, Lafayette College, Easton, Pennsylvania.

[1] a. J. Frenkel, J. Chem. Phys. **7**, 538 (1939); b. A. R. Ubbelohde, Trans. Faraday Soc. **34**, 282 (1938); c. J. W. Oldham and A. R. Ubbelohde, Proc. Roy. Soc. **176**, 50 (1940).

[2] a. G. Egloff, *Physical Constants of Hydrocarbons* (Reinhold Publishing Company, New York, 1939); b. M. P. Doss, *Physical Properties of Hydrocarbons* (Texas Company, New York, 1939); c. G. Calingaert, Beatty, Kuder, and Thomson, Ind. Eng. Chem. **33**, 103 (1941); d. M. R. Lipkin and S. S. Kurtz, Ind. Eng. Chem., Anal. Ed. **13**, 291 (1941); e. R. Deansley and L. T. Carleton, J. Phys. Chem. **45**, 1104 (1941).

[3] J. E. Mayer and S. Streeter, J. Chem. Phys. **7**, 1019 (1939).

[4] The sample of hexadecane whose expansion coefficients are expressed in this report was generously loaned by the Shell Development Company, Emeryville, California. It is the material discussed on pp. 1118–1120 of reference 2e.

[5] F. C. Whitmore and H. H. Johnson, Jr., J. Am. Chem. Soc. **63**, 1481 (1941).

TABLE I. Constants of liquid hydrocarbons.

Hydrocarbon	Density[a] Obs.	Density[a] Standard	Refractive index[a] Obs. n	Refractive index[a] Obs. $-(dn/dt)$	Refractive index[a] Standard n	Refractive index[a] Standard $-(dn/dt)$	Freezing point Obs.	Freezing point Standard	Mole percent Raoult impurities
$C_{14}H_{30}$	0.762	0.7626	1.4290	0.000410	1.4289	0.000440	5.6°	5.5°	0.035
$C_{16}H_{34}$	.773	.7734	1.4344	.000430	1.4345	.000400	18.1	18.145	——
$C_{18}H_{38}$	.782	.7819	1.4388	.000360	1.4390	.000393	28.0	28.0	.190
$C_{24}H_{50}$	.764	.7628	1.4300	.000370	1.4303	.000385	51.1	51.1[b]	.210
	at 76°	at 76°[b]	at 65°		at 65°[b]				

[a] Densities and refractive indices for $C_{14}H_{30}$, $C_{16}H_{34}$, and $C_{18}H_{38}$ are $d_4^{20°}$ and $n_D^{20°}$, respectively; and have been corrected from the temperature of measurement by the coefficients of reference 2e. For $C_{24}H_{50}$ convenient higher temperatures are specified. Standard values are from reference 2e unless otherwise noted. The temperature coefficient of n becomes linear 6–10° above the m.p. These linear values are the ones reported here. Closer to the m.p. the coefficients increase.
[b] See reference 2a.

during the process was first isolated. In this way it is thought that position isomers are largely eliminated,[6] as well as any solid-solid solution formers concentrating preferable in either the solid or liquid phases; and also any contaminating nuclei. Then follow a crystallization (or partial solidification) in which the first fraction is saved, and one in which the last portion is retained. By analogy with the phase diagram for the pair $C_{18}H_{38}-C_{16}H_{34}$,[7] and the observations of Smittenberg, Hoog, and Henkes,[8] this procedure should assist the distillations in eliminating homologs of near molecular weight.

As a result of this extensive purification it is thought that the final samples of tetradecane, octadecane, and tetracosane prepared are as pure as is possible to obtain by present techniques. The only impurities tolerated would be structural isomers not too greatly branched, and neighboring homologs with their structural isomers. These would be present to only small extent in the form of solid-solid solutions[9] with a phase partition coefficient near the unusual value of one.[10] Nevertheless the amounts of impurities were estimated, as Raoult solutes, from the cooling curves, observing the precautions outlined by Mair, Glasgow, and Rossini,[11] and other workers. The results are given in Table I, but lose significance in view of the above discussion, and the experimental observation that samples contaminated with likely impurities do not behave at all as simple solutions. For instance: 1.4 mole percent of hexadecane added to tetradecane actually raised the freezing point 0.3°C, while 0.24 percent $C_{24}H_{50}$ in $C_{18}H_{38}$, and 9.6 percent $C_{18}H_{38}$ in $C_{24}H_{50}$ were indicated as 5.3 and 4.1 percent, respectively. This behavior is typical of solid-solid solution formation; and although the lower paraffins are not generally of this type,[8] there is ample experimental evidence that it prevails amongst the higher neighboring homologs of this series.[1b, 7, 12]

The course of purification was indicated by ordinary capillary melting points. All the pure samples finally obtained were materials which underwent no appreciable change in observed melting point for at least the last three manipulations of the purifying procedure. The freezing points reported were obtained by the cooling curve technique with a directly immersed thermocouple which had been calibrated and compared with a certified Bureau of Standards thermometer. The bromine number of all samples was zero. Standard liquid densities were determined in a small (approximately 1 cc) pycnometer, and are considered as exact only to the third place. An Abbe refractometer was used to ascertain the refractive indices.

As displayed in Table I, the pure samples prepared are at least as pure as the materials for which standard values are accepted.

B. Methods

A one-piece, inverted type dilatometer of well-seasoned Pyrex glass was used. The sample was repeatedly melted and solidified under vacuum,

[6] J. Timmermans, *Chemical Species* (Chemical Publishing Company, New York, 1940).
[7] J. C. Smith, J. Chem. Soc. 737 (1938).
[8] Smittenberg, Hoog, and Henkes, J. Am. Chem. Soc. **60**, 17 (1938).
[9] L. O. Fischer, Bull. Soc. Chim. Belg. **49**, 129 (1940); Chem. Abs. **36**, 324 (1942).
[10] A. E. Hill, Taylor's *Treatise on Physical Chemistry* I (Van Nostrand Company, New York, 1931), p. 556.
[11] Mair, Glasgow, and Rossini, J. Research Nat. Bur. Stand. **26**, 591 (1941).
[12] A. Muller, Proc. Roy. Soc. **127**, 417 (1930); **138**, 514 (1932); **178**, 227 (1941).

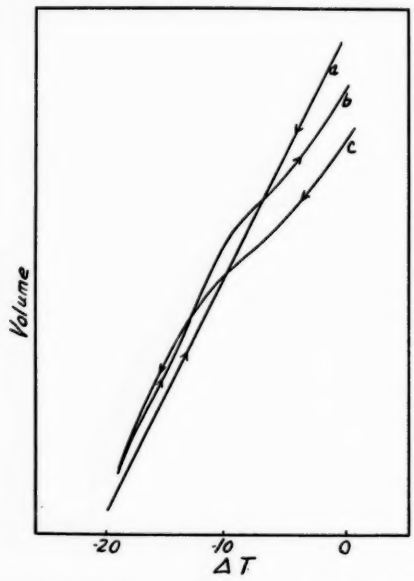

FIG. 1. Typical dilatometric behavior of solid. a, Slowly frozen; b, quickly frozen, warming; c, quickly frozen, cooling.

before and after adding the indicating mercury fluid, in order completely to eliminate entrapped gases. No measurable hysteresis of the dilatometer itself was observed over the complete working range, nor for the hydrocarbons over their liquid temperature ranges. For any particular slowly frozen hydrocarbon the volume recorded, as the temperature was varied below the freezing point, was remarkably duplicable. For more quickly frozen samples hysteresis becomes greater as the freezing gradient is increased. The hysteresis is of the type illustrated in Fig. 1, and is to be explained by the minute cracks and fissures produced upon solidification. These are more abundant and less regular for the less perfectly formed crystals. While the slowly produced crystals are not free from such defects (evidenced by the translucency and by the densities of Table II), apparently the vacuoles and interstices are consistently uniform and quite efficiently occupied and vacated by the mercury during temperature variation. The results reported for the solid states are for slowly grown solids.

From the weight of sample used in each determination, the density at any condition could be computed from the characteristics of the instrument. Although such values do not have the accuracy of the pycnometer determinations, they do supply approximate values of the densities of the solids, and their temperature variations. Since such data are not available in the literature the approximate values observed are reported in Table II. These values have been used in calculating the coefficients of thermal expansion.

C. Methods

The results are presented in Figs. 2–5, as thermal expansion coefficients $\alpha=[(\partial V/\partial T)_P/V]$. (Δ_T) in these plots represents the temperature difference from the melting points. The points shown represent only part of many observed values; many of these are rest or true equilibrium values, especially in the neighborhood of melting. Some extreme values are also shown.

On these same plots are shown some representative results for purest material deliberately contaminated with what are considered likely impurities. It is apparent that amounts of contaminant less than about 2 percent (which is much more than the probable impurity present in the pure samples) have no effect on the expansion of the solid. Larger amounts lead to lowered transition temperatures. The effect of slight impurity on the liquid side is not very disturbing, but with a suggestion of the elimination of the tendency toward a minimum displayed by the original curves. Larger amounts increase the slope of the liquid expansion curves.

DISCUSSION

A. Solid Side of the Transition

From Ubbelohde's[1b] results on the specific heat of octadecane it was expected that any disordering of the solid would be more manifest than the reciprocal ordering of the liquid as the melting or freezing point is approached. However two serious objections vitiate the explanation of this

TABLE II. Approximate densities of solid hydrocarbons.

Hydrocarbon	Density, 10° below m.p.	Density calc.[a]	α, 10° below m.p.	Total molar volume change on melting
$C_{24}H_{30}$	0.85[b]	0.89	6×10^{-4}	42.0 cc
$C_{16}H_{34}$	.91	.91	7.5	45.7
$C_{18}H_{38}$	.86	.92	4	40
$C_{24}H_{50}$	.87[c]	.93	6[c]	51

[a] See reference 12.
[b] Ubbelohde (reference 1b) reports 0.870 at 0°C.
[c] 20° below the m.p. At $(\Delta t) = -4$, the observed density is 0.79.

observed behavior as a disordering phenomenon. These are the inevitable presence of even slight amounts of impurity (an effective objection to both the specific heat and expansion results), and the imperfect growth of the solid as a continuous, perfect, single crystal.

While the amount of impurity in each sample has been reduced to a minimum, and is much less than that estimated as necessary completely to describe the observed behavior, it is not thus irrevocably eliminated since localized concentrations are very likely in the solid state. However, the comparative results on contaminated compounds reveal that premelting due to similar impurities is not significant. Microscopic observation of samples frozen under mercury reveals that many of the minute cracks and fissures are incompletely occupied by the indicating fluid, and it is considered likely that the large effect noticed on the solid side of the transition is due largely to this behavior. Incomplete occupation is also observed in the case of hexadecane, in which the agreement of observed and calculated densities suggests a complete filling of these spaces.

While the experimental work reported is in complete accord with Ubbelohde's observations, it does not unalterably validate his explanation as a disordering phenomenon because of the coupled effect of these two factors. However the dielectric and x-ray studies of Muller[12] on these and similar compounds indicate that there is an inordinate expansion of these lattices prior to melting. The x-ray studies in particular are free of the objections mentioned, and therefore emphasize the explanation suggested by various workers.[2b,13] These objections are also minimized or absent on the liquid side of the transition, and the results there are considered a more positive indication of an order-disorder mechanism of freezing-melting.

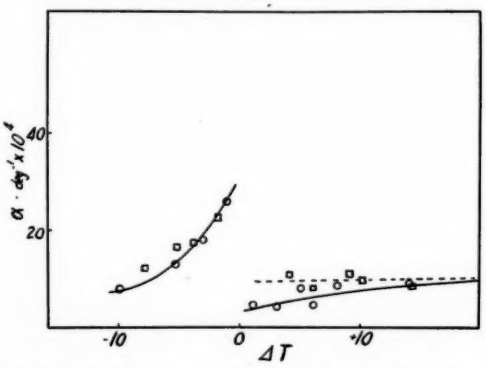

FIG. 2. $C_{14}H_{30}$; ○, pure sample; □, contaminated with 1.4% $C_{16}H_{34}$; – – –, standard value (reference 2e).

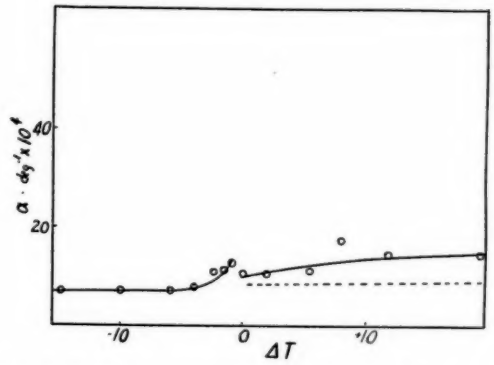

FIG. 3. $C_{16}H_{34}$; – – –, standard values (reference 2e).

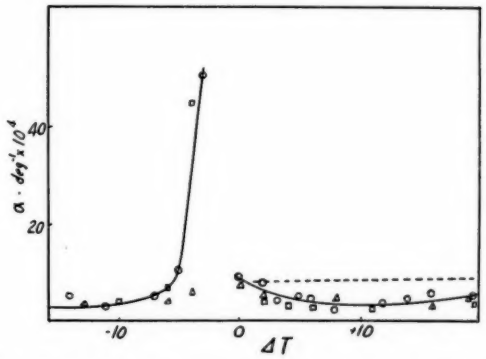

FIG. 4. $C_{18}H_{38}$; ○, pure sample; □, contaminated with 0.36% $C_{24}H_{50}$; △, contaminated with 1.98% $C_{24}H_{50}$; – – –, standard values (reference 2e).

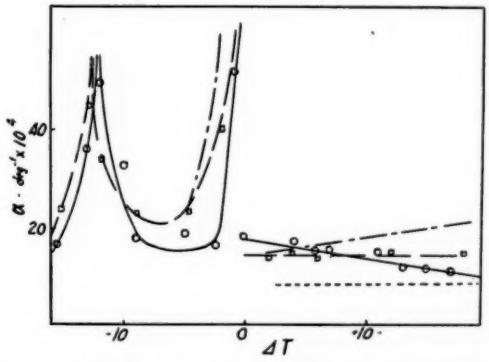

FIG. 5. $C_{24}H_{50}$; ○, pure sample; — —, contaminated with 7.1% $C_{18}H_{38}$; — — —, contaminated with 7.1% $C_{18}H_{38}$, plus 2.5% residue from first crystallization; – – –, standard values (reference 2a).

[13] O. K. Rice, J. Chem. Phys. 7, 887 (1939).

B. Liquid Side of the Transition

The expansion data for the liquid phases is in accord at particular temperatures with the standard values available for these hydrocarbons. The present data indicate a variation not revealed by the usual linear temperature dependence. By analogy with the more complete and exact information about lower paraffins,[2c, d] it is expected that the coefficients a, b, and c in the empirical density equation

$$d=d_0-af(T)+bf(T^2)+cf(T^3) \qquad (2)$$

will progressively decrease, increase, and increase, respectively, as the series is ascended. This behavior should develop a change in slope in the density- (or thermal expansion coefficient) temperature curves; and it is this behavior which is revealed here for octadecane and indicated for the others.

In terms of structure the compacting of the liquid state will be due chiefly to diminished thermal activity; but in addition there may develop additional contraction because of greater symmetrical arrangement, or greater internal rigidity, of the molecules. Such an ordering of the liquid state is amply indicated by a wide variety of experimental studies,[14] and the density behavior reported here is entirely in harmony with that picture.

The effect of impurity, small as it might be, is not as significant on the liquid side of the transition as on the solid side, since the possibility of localized concentrations is absent.

C. Gruneisen's Law

The general thermodynamic equality (1) has been simplified in the form of the semi-empirical Gruneisen's law, which states that the ratio of C_v to α for a solid is essentially a constant. Many substances, chiefly metals, are known to follow this relation even close to their melting points, although exceptions are numerous.[15] While the quantum-mechanical background of the law does not suggest applicability in the case of mobile molecules, it was nevertheless tested for these hydrocarbons. Ubbelohde's specific heat data and the present expansion coefficients were employed. The former were converted to C_v values by means of the relation; $C_p-C_v=TV(\alpha^2/\beta)$ where V is the molar volume, and β the compressibility, assumed constant. The results were not even in approximate agreement with Gruneisen's law.

SUMMARY AND CONCLUSIONS

Thermal expansion data about the melting temperatures for pure and deliberately contaminated tetradecane, hexadecane, octadecane, and tetracosane are presented.

The changes in volume as melting and freezing are approached suggest an order-disorder mechanism for the transition.

The liquid side of the transition is more free of secondary influences than the solid side.

[14] a. A. R. Ubbelohde, Ann. Reports 168–171 (1940); b. Symposium; Trans. Faraday Soc. **33**, 1–114 (1937).

[15] J. C. Slater, *Introduction to Chemical Physics* (McGraw-Hill, 1939), p. 219.

Letters to the Editor

THIS section will accept reports of new work, provided these are terse and contain few figures, and especially few halftone cuts. The Editorial Board will not hold itself responsible for opinions expressed by the correspondents. Contributions to this section should not exceed 600 words in length and must reach the office of the Managing Editor not later than the 15th of the month preceding that of the issue in which the letter is to appear. No proof will be sent to the authors. The usual publication charge ($3.00 per page) will not be made and no reprints will be furnished free.

Surface Tension of Micelle-Forming Solutions

A. E. ALEXANDER
Colloid Science Department, Cambridge, England
August 26, 1942

THE recent communication by Cassel[1] on this much-discussed topic agrees, on the whole, with the conclusions arrived at by the present author in a note of last year,[2] and since amplified into a more detailed and general form.[3]

In these publications the earlier views of other authors[4] were examined and rejected, and a quite general treatment, still based upon that of Gibbs, was shown to be in accord with experiment. The vanishing of $d\gamma/dC$ (as at the minimum of surface tension), was very simply explicable on the basis of micellar aggregation.

While in general agreement with Cassel, the writer would disagree somewhat with his last paragraph, in which a crystalline or liquid-crystalline structure is assigned to the adsorbed surface films, and a superposition of surface tension and surface stress is suggested as possibly responsible for time effects before the minimum surface tension is reached.

In a recent paper on the structure of the surfaces of solutions,[5] it was pointed out that the adsorbed films are most certainly of the compressed gaseous type, and that the area occupied by each molecule at the minimum surface tension is of the order of 50 percent greater than that possible on the basis of close-packed hydrocarbon chains. Thus the adsorbed films definitely cannot be classed as crystalline, nor even as liquid-crystalline save insofar as all highly compressed gaseous films possess a considerable degree of molecular orientation.

With regard to the time effects occurring before the minimum surface tension is reached, the explanation suggested some time ago,[6] admittedly a tentative one but in terms of a definite molecular mechanism, seems preferable to a rather vague phrase such as that quoted above.

[1] H. M. Cassel, J. Chem. Phys. **10**, 246 (1942).
[2] A. E. Alexander, Nature **148**, 752 (1941).
[3] A. E. Alexander, Trans. Faraday Soc. **38**, 248 (1942).
[4] R. F. Nickerson, J. Phys. Chem. **40**, 277 (1936); N. K. Adam, Physics and Chemistry of Surfaces (O. U. Press) third edition, p. 408; J. W. McBain and G. F. Mills, Reports on Progress in Physics **5**, 30 (1939); F. A. Long and G. C. Nutting, J. Am. Chem. Soc. **63**, 625 (1941).
[5] A. E. Alexander, Trans. Faraday Soc. **38**, 54 (1942).
[6] A. E. Alexander, Trans. Faraday Soc. **37**, 15 (1941).

Nature of the Covalent Binding

THEODORE BERLIN* AND KASIMIR FAJANS
Department of Chemistry, University of Michigan, Ann Arbor, Michigan
October 14, 1942

IT has been found advantageous to consider the binding within di- and polyatomic covalent particles as due to the interaction of electrons and charged atomic cores rather than to an interaction between neutral atoms.[1]

This emphasis on the electric interaction throws additional light on the binding within H_2^+ and H_2, already so successfully clarified by wave mechanics.[2]

For comparison, we apply to H_2^+ the assumptions used in Niels Bohr's[3] treatment of the hydrogen molecule. 1. Coulomb forces are the only source of the molecular potential energy. 2. Classical mechanics applies to the motion of the electron considered as permanently symmetrical to both protons; speed v, radius of the circular orbit a. 3. $mva = nh/2\pi$.

On this basis, $E = -11.9$ ev ($n = 1$) results for the binding energy $2H^+ + e^- = H_2^+$. The experimental value is -16.3 ev, with which the wave mechanical value is in full agreement. It should be emphasized that in the wave mechanical treatment the potential energy is also purely Coulombic. However, contrary to assumption 2, the density of negative electricity proves to be distributed symmetrically with respect to both protons only on the time average, which gives rise to a temporary dipole moment of H_2^+.

This temporary asymmetry makes the potential energy V of H_2^+ with respect to $2H^+$, e^- lower than it would be in the permanently symmetrical Bohr model. For the latter: $V = -23.8$ ev, the kinetic energy $E_k = 11.9$ ev. Calculations on the basis of wave mechanical variation functions of H. M. James or of V. Guillemin and C. Zener[4] give the average potential energy $V = -32.6$ ev, the average $E_k = 16.3$ ev.

In the case of the binding energy of the hydrogen molecule ($2H^+ + 2e^- = H_2$), the situation is qualitatively the same. When both electrons would move permanently symmetrically to both protons, $E = -29.9$ ev. The corresponding experimental value is $E = -31.8$ ev. The binding energy is again larger, but only by 6.4 percent, while in the case of H_2^+ the difference between 11.9 and 16.3 is 37 percent. Obviously, the temporary deviations from the average symmetrical position are smaller for H_2, with its two electrons and internuclear distance $r = 0.74$A, than for the single electron of H_2^+ and $r = 1.06$A.

The above considerations prove to be useful when applied to Li_2. The binding energy ($2Li^+ + 2e^- = Li_2$) is $E = -11.9$ ev, the internuclear distance $r = 2.67$A. The difference between H_2 and Li_2 is due to the fact that Li^+ has an electronic shell. The electron distribution curve for Li^+ indicates that at the internuclear distance of H_2 (0.74A), the electronic systems of the two Li^+ would considerably overlap, and the repulsion between the excess charges would be increased by that of the electronic shells. At the distance 2.67A, the latter can be neglected. Based on Bohr's model, treating Li^+ as a point charge, the large difference in r and E of H_2 and Li_2 could be due only to a different value of n in assumption 3. Putting $n = 2$; $r = 2.33$A and $E = -7.5$ ev.

By analogy with H_2^+ and H_2, the large relative difference between 7.5 and 11.9 ev can be interpreted as due to the asymmetry of the motion of the electrons of Li_2, enhanced by the large internuclear distance 2.67A.

Hence, to the above emphasis that the binding in the covalent molecules H_2^+, H_2, Li_2, which do not have a permanent dipole moment, is caused by Coulombic forces, one has to add that part of the potential energy is due to the temporary polarity of the molecules. The Bohr model represents the idealized permanently unpolar binding. While the idealized binding between rigid ions is an electrostatic phenomenon, the idealized and the real covalent bindings are electrokinetic in nature.

*Horace H. Rackham Predoctoral Fellow, 1941–1942 and 1942–1943.

[1] See abstracts of our papers presented at the Buffalo Meeting of the American Chemical Society on September 10, 1942. The detailed publication will follow soon.

[2] H_2^+: O. Burrau, Kgl. Danske Vid. Sels. Math-Fys. Medd. **7**, 1 (1927); E. A. Hylleraas, 1931; G. Jaffé, 1934. H_2: H. M. James and A. S. Coolidge, J. Chem. Phys. **1**, 825 (1933).

[3] N. Bohr, Phil. Mag. **26**, 857 (1913).

[4] See L. Pauling and E. Bright Wilson, *Introduction to Quantum Mechanics* (McGraw-Hill Book Company, New York, 1935), pp. 332–333.

On the Structure of a Metal During Deformation

DAVID HARKER
General Electric Company, Schenectady, New York
August 21, 1942

THE cold working of a metal must produce extreme disarrangement of the orderly atomic array known to exist in metals. Even a short time after as violent a distortion as 90 percent rolling a metal consists of crystallites—each of which contains several million atoms in a quite orderly pattern[1]—although practically every atom must have changed at least some of its neighbors. However, the mechanism by which the originally crystalline metal passed through the deforming process, to become, finally, crystalline again, is still in question.

In order to study the structure of a metal during deformation, the following simple experiment was performed: A hardened steel edge was clamped in the center of a cylindrical x-ray diffraction camera so that the edge could serve as a powder specimen. A copper ribbon was bent around this edge and pulled so that it traveled over the edge continuously. During the motion of the copper ribbon, the edge could be irradiated with x-rays and the diffraction pattern recorded on a photographic film in the usual way. This apparatus is diagramed in Fig. 1. A piece of carefully annealed copper ribbon 0.1 mm thick was made very hard and springy by one pass over the edge, so that considerable work hardening and, therefore, distortion must have been given the metal during this process. Two kinds of diffraction pattern were made: one with the copper ribbon bent around the edge, but not moving; the other with the copper ribbon traveling over the edge at about four centimeters a second. The two kinds of pictures turned out to

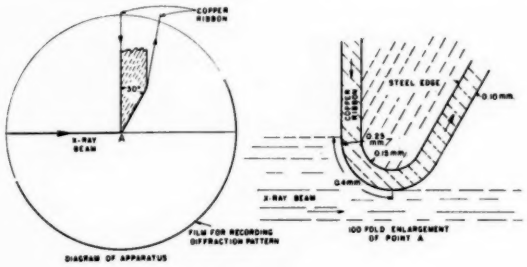

FIG. 1.

be indistinguishable—both showed only the lines of cold-worked copper with the same positions, intensities, and widths.

W. L. Bragg[2] has a picture of the behavior of metals during deformation from which my result could have been predicted. According to this picture, crystallites will grow very rapidly from an amorphous mass of metal until they reach a certain minimum size. My result insures that not more than one-tenth of the copper irradiated was non-crystalline, and also that the crystalline material present was of about the same particle size and state of strain, whether the copper ribbon had been deformed one one-hundredth of a second or several minutes previously. Crudely, one could say that, according to this experiment, a metal recrystallizes as fast as it is deformed.

The possibility of finite thicknesses of amorphous, or "vitreous," metal seems very faint indeed, in view of the results just described.

[1] W. A. Wood, Proc. Phys. Soc. **52**, 111 (1940).
[2] W. L. Bragg, Proc. Phys. Soc. **52**, 108 (1940).

Erratum: The Diffraction of X-Rays by Liquid Oxygen

(J. Chem. Phys. **10**, 504 (1942))

P. C. SHARRAH AND N. S. GINGRICH
University of Missouri, Columbia, Missouri

Temperatures in Figs. 2a and b are incorrect. They should read: Fig. 2a, 89°K in place of 62°, and 62° in place of 85°; Fig. 2b, 89°K in place of 85°.